Simulations of binary neutron stars and black hole-torus systems in general relativity

José A. Font

Departamento de Astronomía y Astrofísica

VNIVERSITAT DE VALÈNCIA

Why study binary neutron star mergers?

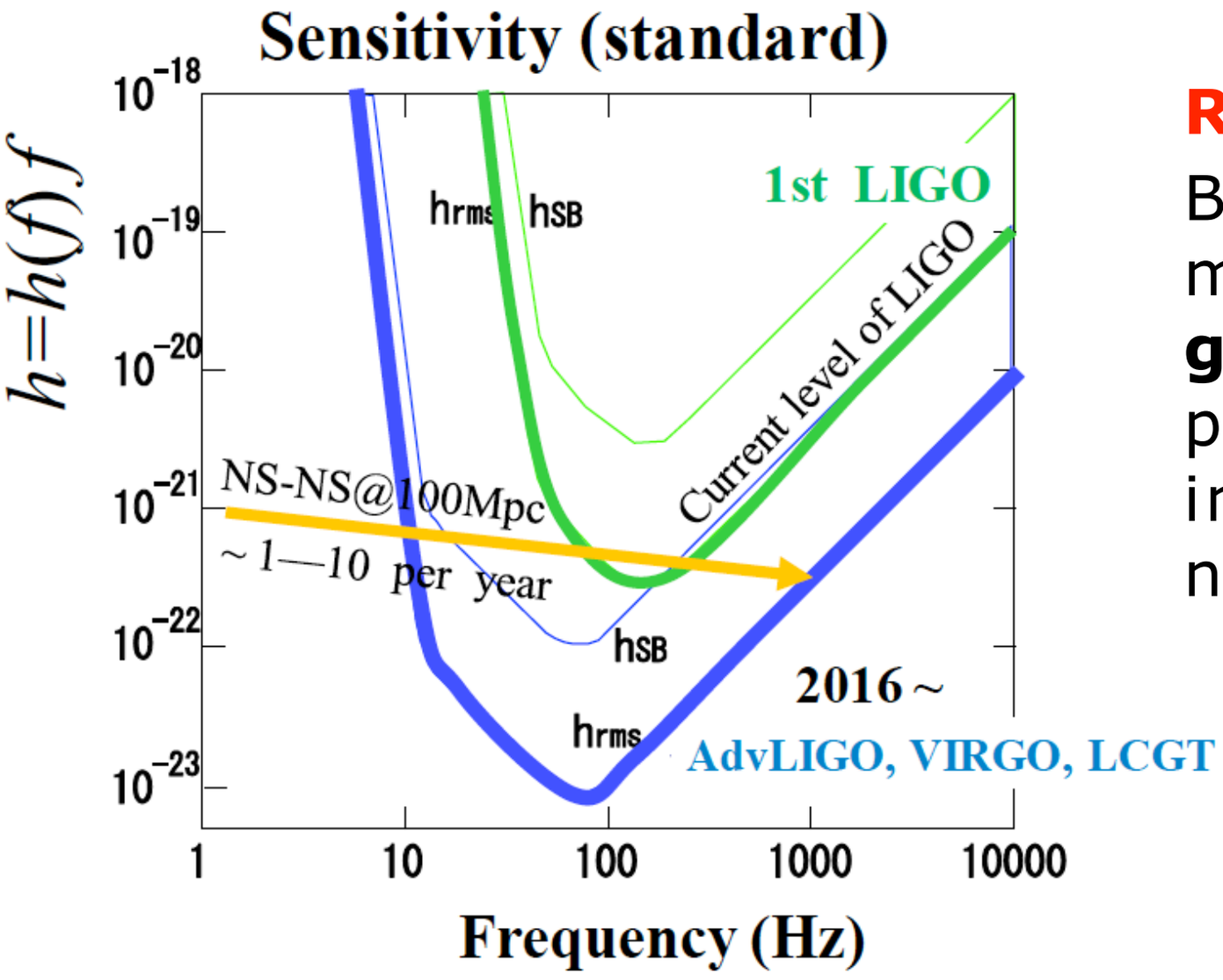

Reason #1:

Because they are among the most powerful sources of **gravitational waves.** Could provide key information to improve understanding of neutron star physics and EOS.

BNS & BH-NS mergers = GW source

Before merger ($10 < f <$ ~kHz)

after merger ($f >$ ~kHz)

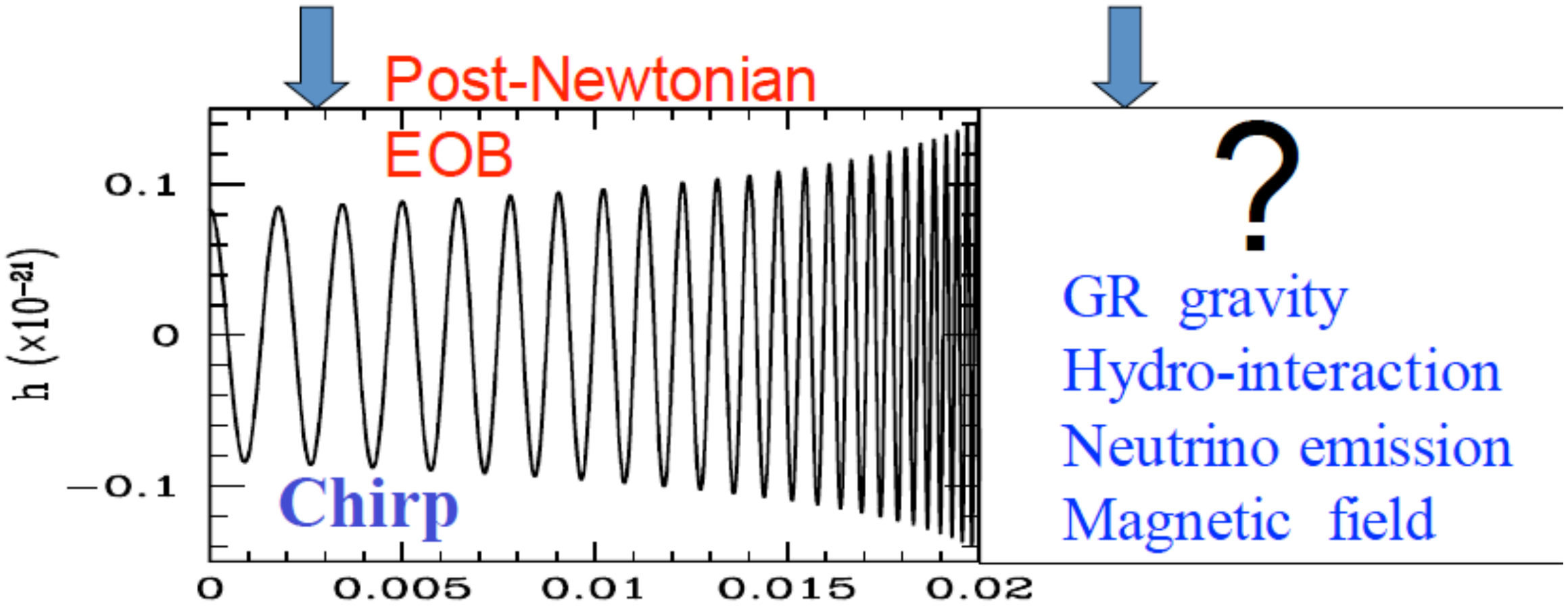

?

GR gravity

Hydro-interaction

Neutrino emission

Magnetic field

Numerical relativity

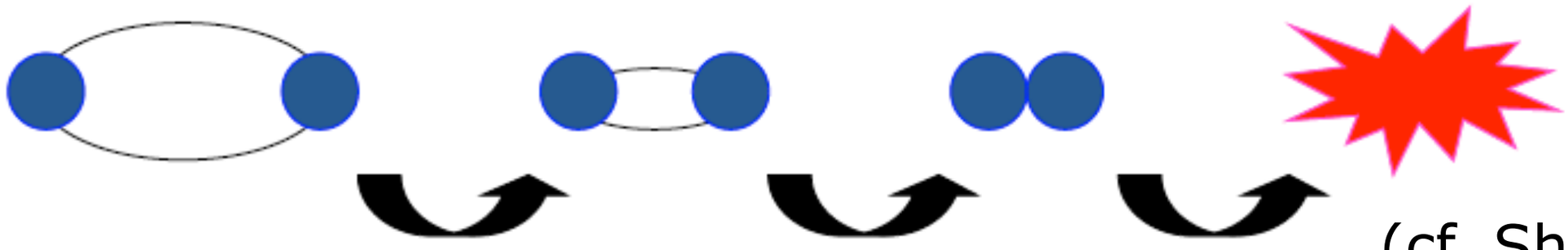

(cf. Shibata)

Why study binary neutron star mergers?

Reason #2: Excellent laboratory to study high-density nuclear physics (key to decipher the NS physics)

Neutron star composition still unknown

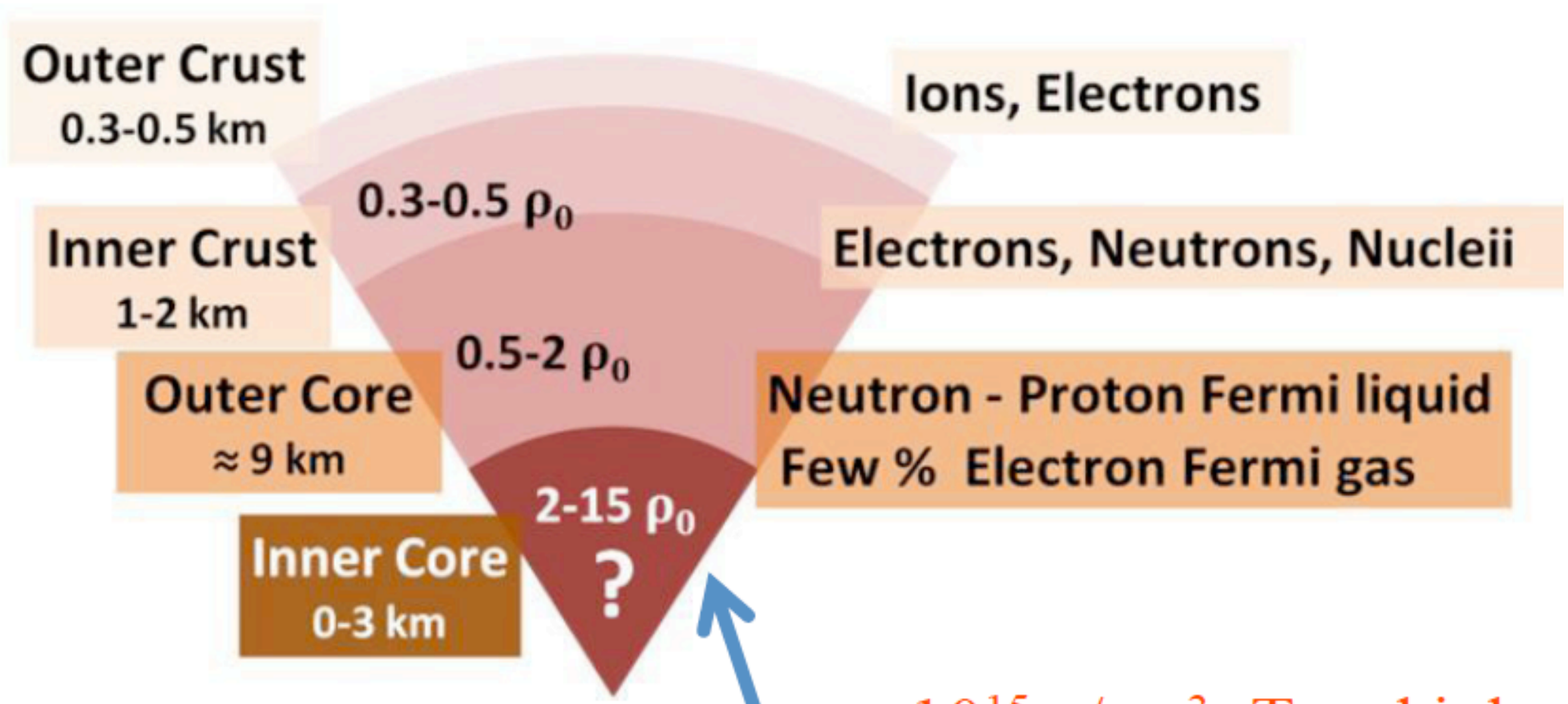

ρ_0=2.8*10^{14} g/cm^3

$\rho \sim 10^{15}$ g/cm^3: Too high

Components: Neutron + ?????

Radius: 10—15 km ?

Many different possibilities depending on the EOS

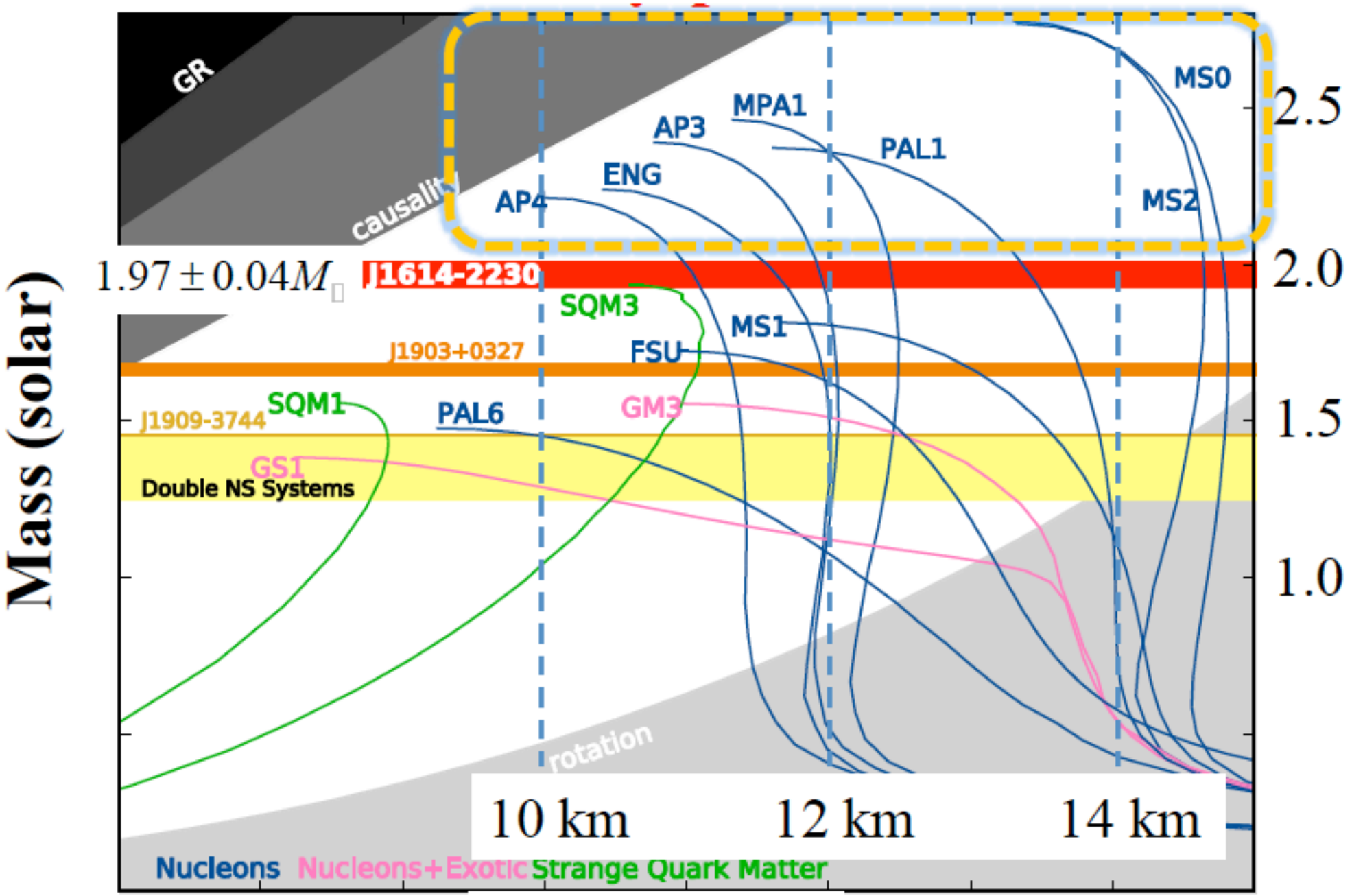

(cf. Prof. Blaschke's talk)

Demorest et al (2010)

GWs in the late inspiral and merger phases could constrain NS EOS.
Many GW templates from Numerical Relativity are necessary

Why study binary neutron star mergers?

Reason #3:

Because their inspiral and merger could be behind one of the most powerful phenomena in the universe: **short Gamma Ray Bursts** (GRBs)

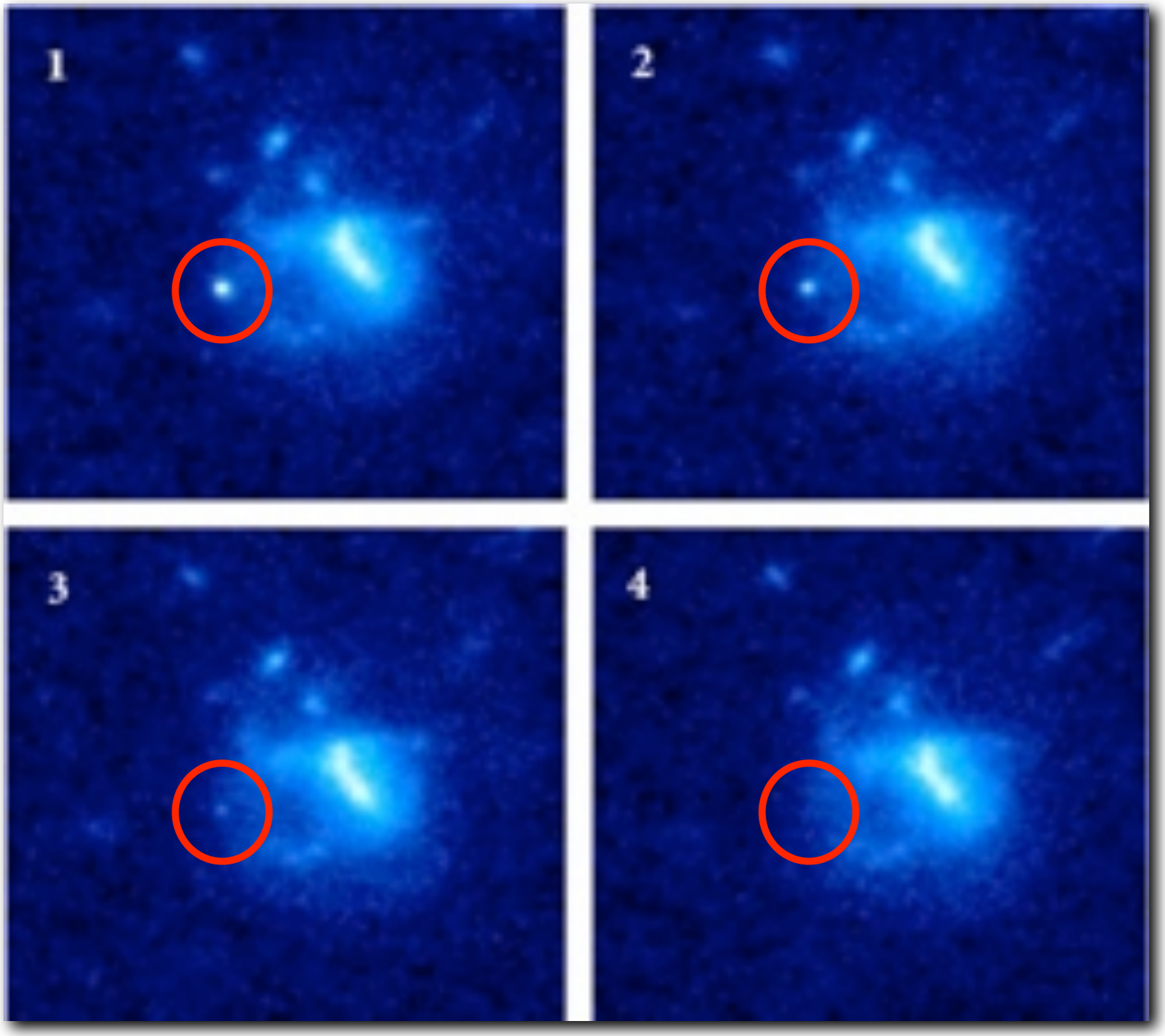

HST images of July 9, 2005 GRB taken 5.6, 9.8, 18.6 & 34.7 days after the burst (Derek Fox, PSU)

Standard channel for BNS (or BH/NS) formation

Merging BNS form through similar evolutionary channels in stellar field populations of galaxies.

Population synthesis calculations favour standard channel in which the first-born compact object goes through a CE phase.

CE/Giant phase

Dynamical friction shrinks binary separation; sufficient energy released to expel envelope

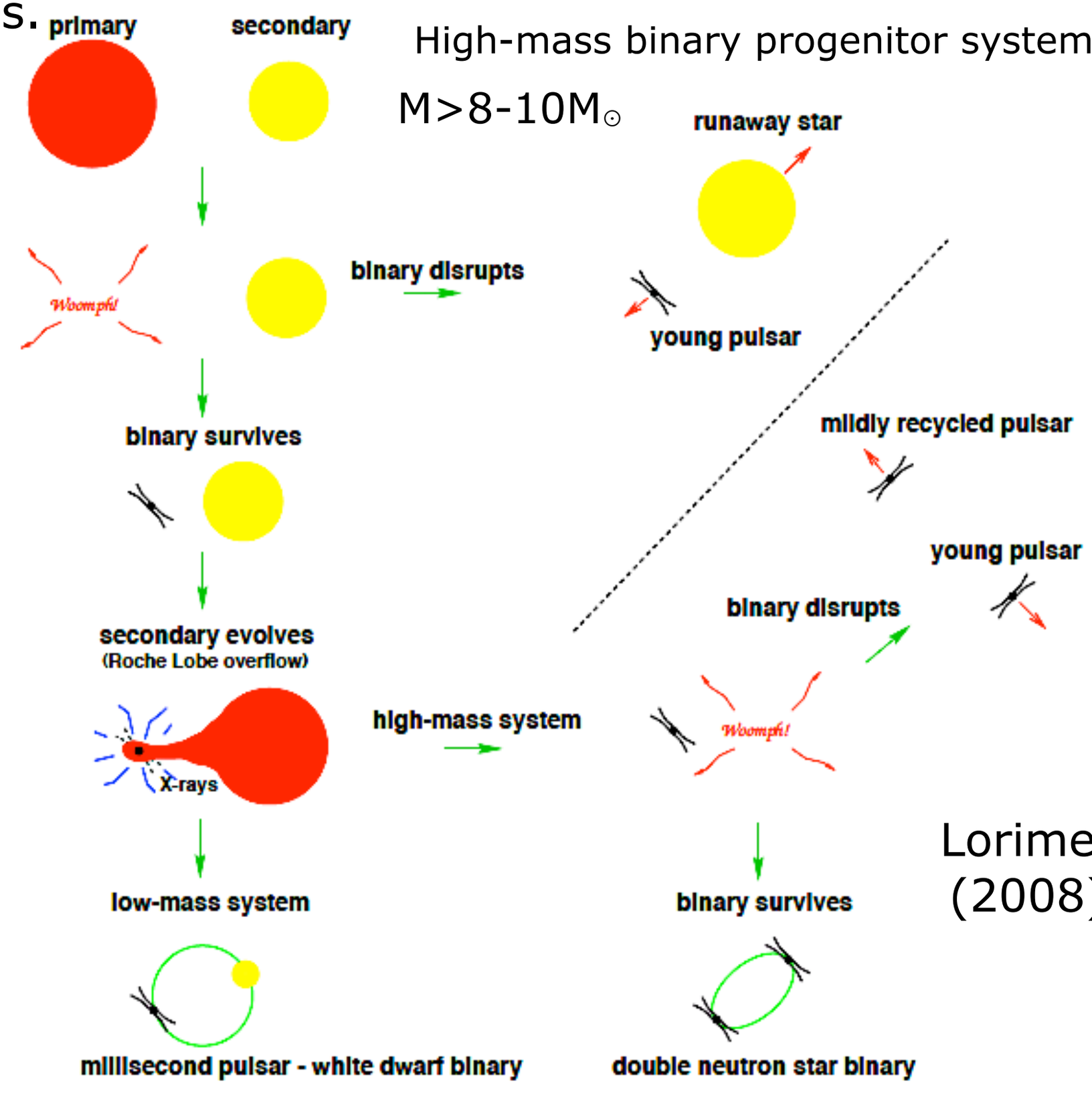

Lorimer (2008)

Evolution of BNS

Inspiral

Formation
(after two supernovae)
Evolve as a result
of GW emission

Last 1 hour at $r \sim 1000$ km
$f_{GW} \sim 7$ Hz

Merger starts when
$r \sim 30$ km ($f_{GW} \sim 1$ kHz)

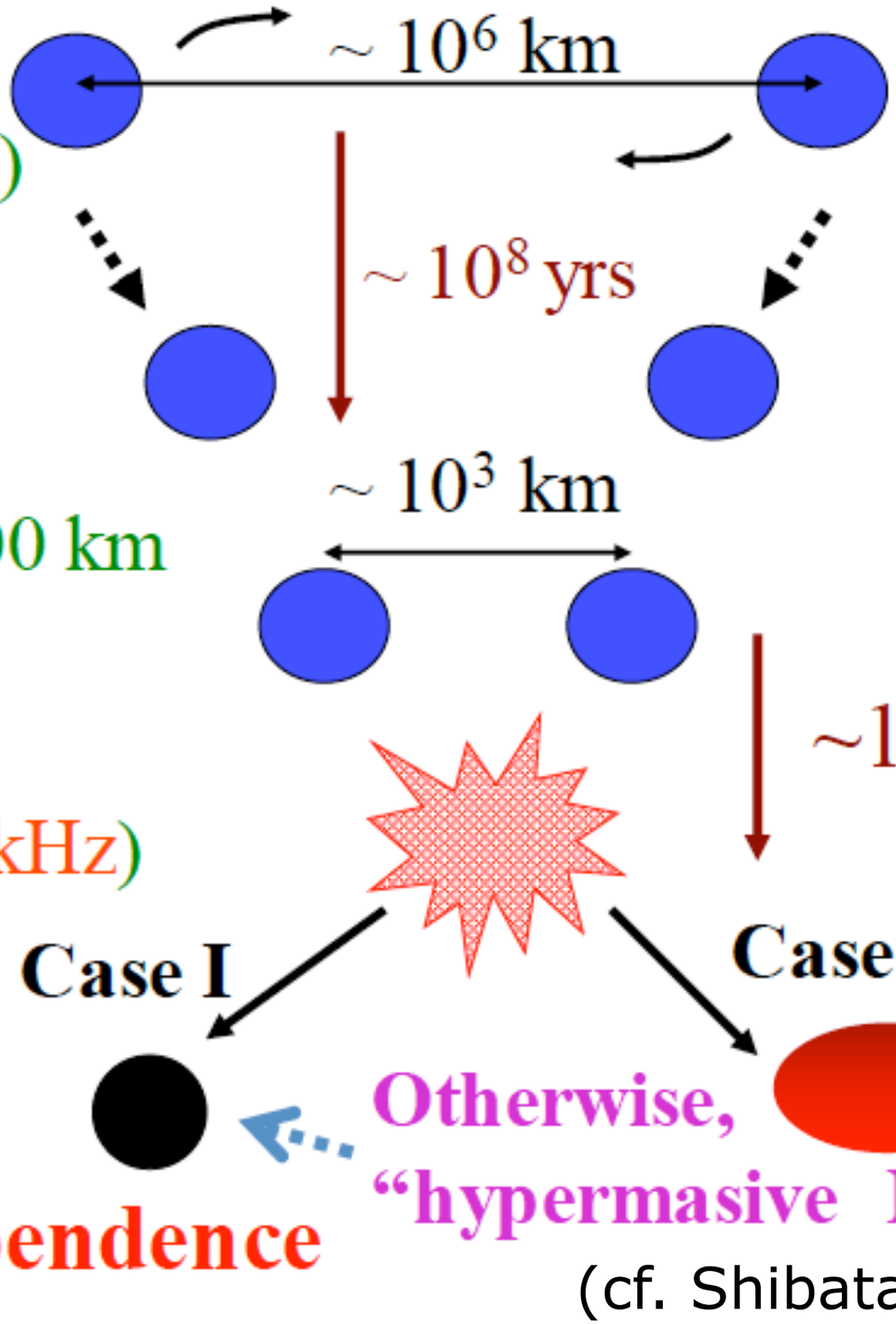

**If mass is high enough,
a black hole is formed**

Large EOS-dependence

(cf. Shibata)

Galactic compact BNS observed

	PSR	P(day)	e	$M(M_{\rm sun})$	M_1	M_2	$T_{\rm GW}$
1.	B1913+16	0.323	0.617	2.828	1.387	1.441	2.45
2.	B1534+12	0.421	0.274	2.678	1.333	1.345	22.5
3.	B2127+11C	0.335	0.681	2.71	1.35	1.36	2.2
4.	J0737-3039	0.102	0.088	2.58	1.35	1.24	0.85
5.	J1756-2251	0.32	0.18	2.58	1.31	1.26	1.69
6.	J1906-0746	0.166	0.085	2.62	1.25	1.37	3.0

[according to lowest-order dissipative contribution from GR (2.5PN level); both NSs point masses.]

10^8 yrs

$$\tau_{\rm GW} = \frac{5}{64}\frac{a^4}{\mu M^2} = 2.2\times 10^8 q^{-1}(1+q)^{-1}\left(\frac{a}{R_\odot}\right)^4\left(\frac{M_1}{1.4M_\odot}\right)^{-3}\ {\rm yr}$$

Merger time

6 (GC) NS-NS, which will merge within a Hubble time (13.7 Gyr), have been found.

see Lorimer (2008)

Detection rate by population synthesis

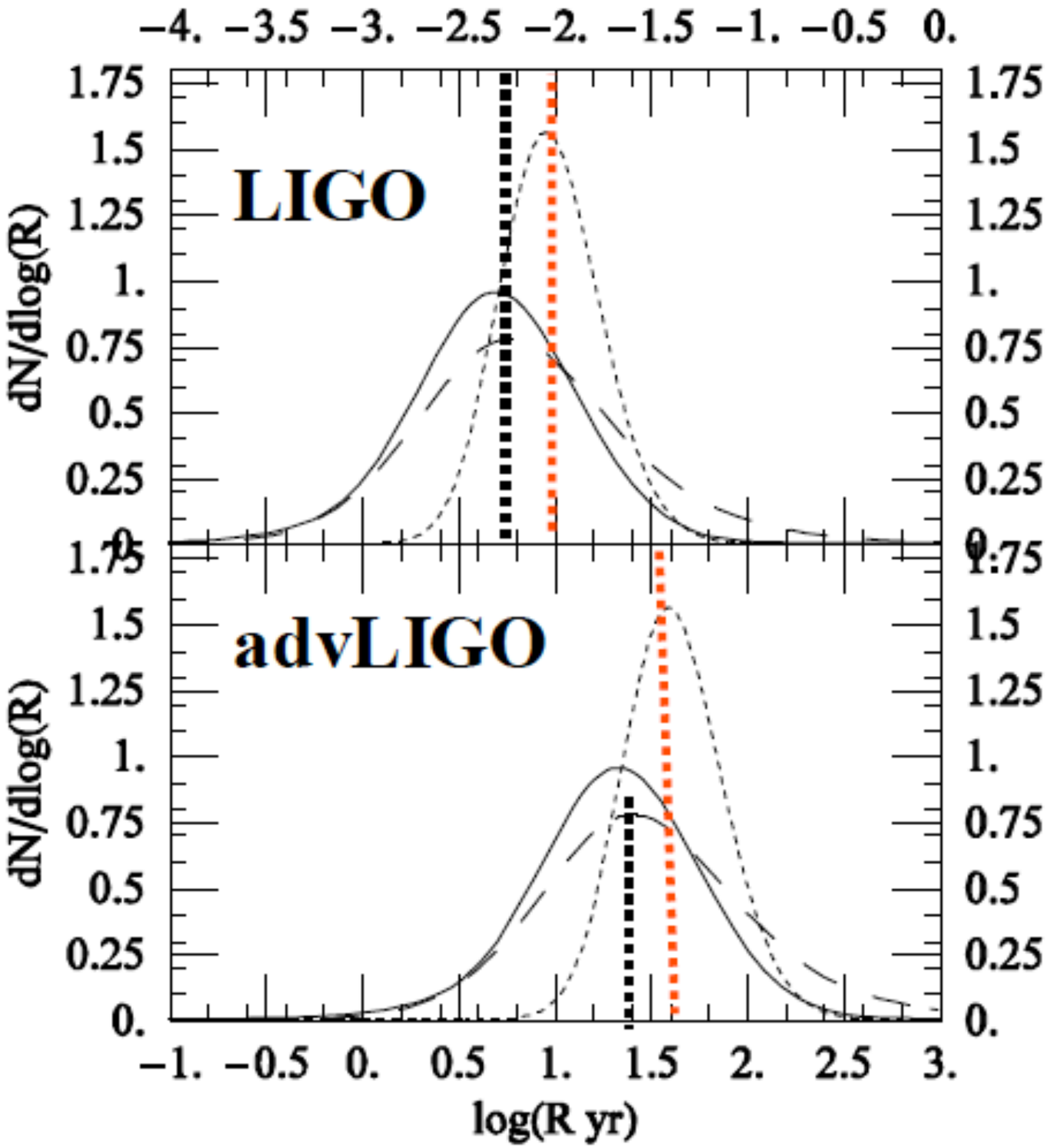

dot： NS/NS

solid： BH/NS

dashed: BH/BH

NS/NS

- 10^{-3}-10^{-1} per year for LIGO
- $10^{0.6}$-$10^{2.6}$ per year for advLIGO

Kalogera et al 2007

Numerical relativity simulations of BNS

Current state of the art

$$R_{\mu\nu} - \tfrac{1}{2} g_{\mu\nu} R = 8\pi T_{\mu\nu} \qquad (\text{field eqs}: \ 6+6+3+1)$$

$$\nabla_\mu T^{\mu\nu} = 0 \ , \qquad (\text{cons. en./mom.}: \ 3+1)$$

$$\nabla_\mu (\rho u^\mu) = 0 \ , \qquad (\text{cons. of baryon no}: \ 1)$$

$$p = p(\rho, \epsilon, \ldots) \ . \qquad (\text{EoS}: \ 1+\ldots)$$

Ongoing improvements on the physics: EoS, neutrino processes, magnetic fields, dissipative fluids, radiative transfer, ... New Frontier

$$\nabla^*_\nu F^{\mu\nu} = 0, \ (\text{Maxwell eqs.}: \ \text{induction}, \ \text{zero div.})$$

$$T_{\mu\nu} = T^{\text{fluid}}_{\mu\nu} + T^{\text{em}}_{\mu\nu} + \ldots$$

Existing numerical work on BNS mergers

The numerical investigation of the coalescence and merger of binary neutron stars within the framework of general relativity is receiving increasing attention in recent years (e.g. Shibata & Taniguchi 2006, Anderson et al 2008, Baiotti et al 2008, 2009, Liu et al 2008, Giacomazzo et al 2009, Kiuchi et al 2009, Rezzolla et al 2010).

Drastic **improvements** in the simulation front regarding **mathematics** (e.g. formulation of the equations), **physics** (e.g. incorporation of EOS from nuclear physics and MHD), and **numerical methods** (e.g. use of high-resolution methods and adaptive mesh refinement), along with increased **computational resources**, have allowed to extend the scope of the early simulations (e.g. Shibata and Uryu 2000).

Larger initial separations have recently started being considered and some of the existing simulations have expanded the range spanned by the models well beyond black-hole formation (Baiotti et al 2008, Kiuchi et al 2009, Giacomazzo et al 2009, Rezzolla et al 2010).

This talk: cold EOS simulations; no thermal EOS or neutrino effects.

Numerical framework for the simulations

Gravitational field eqs (www.cactuscode.org)

Use a conformal and traceless "3+1" formulation of Einstein equations

Gauge: "1+log" slicing for lapse; hyperbolic "Gamma-driver" for shift

Use consistent configurations of irrotational binary NSs in quasi-circular orbit

Use 4th-8th order finite-differencing

Wave-extraction with Weyl scalars and gauge-invariant perturbations

Hydrodynamics/MHD eqs (www.whiskycode.org)

Riemann-solver-based HRSC TVD methods (HLLE, Roe, Marquina) with high-order cell reconstruction (minmod, PPM)

Method of lines for time integration

Use excision if needed

Divergence-free magnetic field condition (CT, divergence cleaning)

AMR with moving grids (www.carpetcode.org)

Equal-mass BNS merger

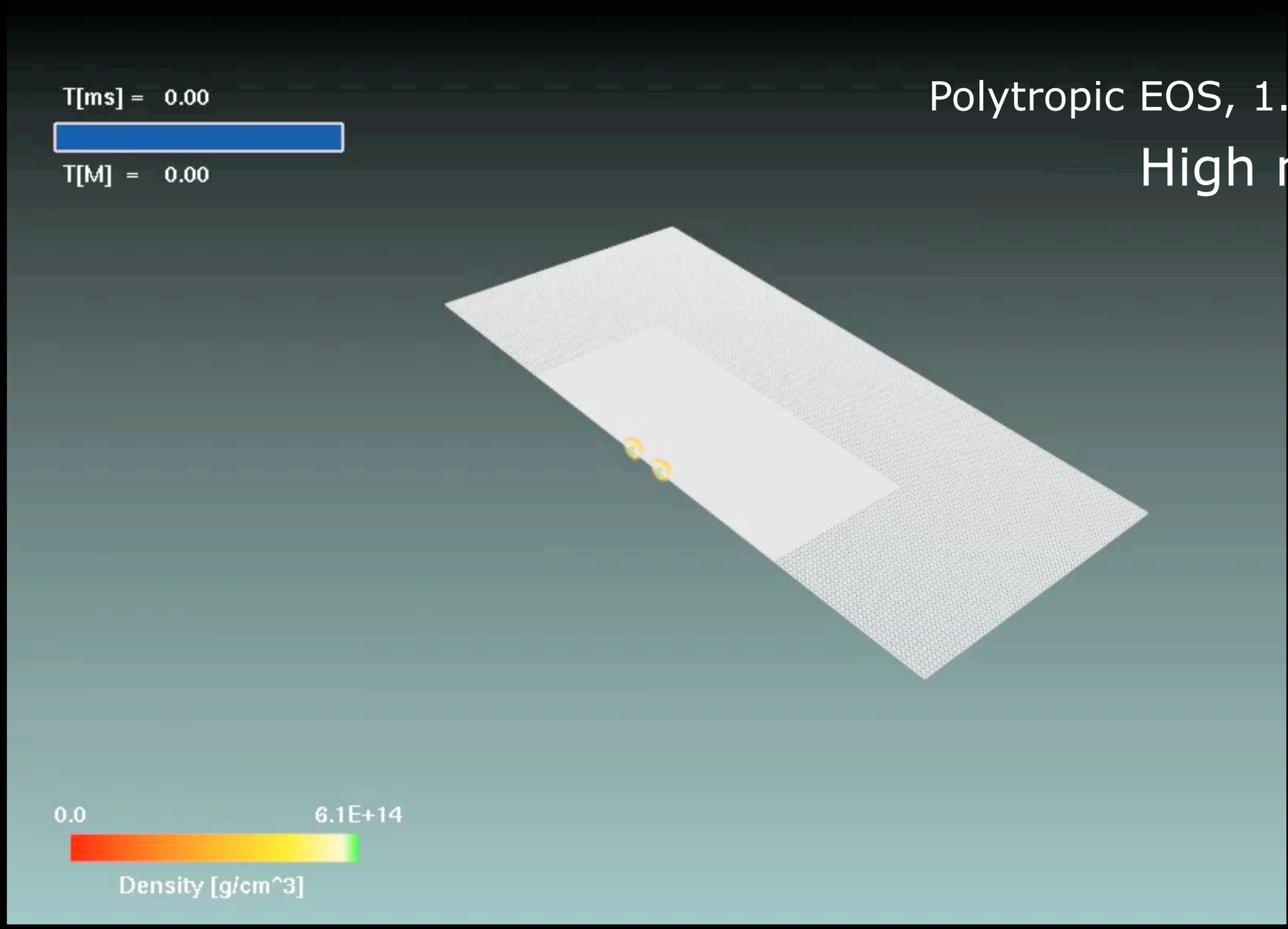

A hot, low-density torus is produced orbiting around the BH.
This is what is expected in short GRBs.

(Baiotti et al 2008)

The behaviour:

BNS merger ⟶ HMNS ⟶ BH+torus

is general but only qualitatively

Quantitative differences are produced by:

- differences in the mass for the same EOS:

a binary with smaller mass will produce a HMNS which is further away from the stability threshold and will collapse at a later time

- differences in the EOS for the same mass:

a binary with an EOS allowing for a larger thermal internal energy (ie hotter after merger) will have an increased pressure support and will collapse at a later time

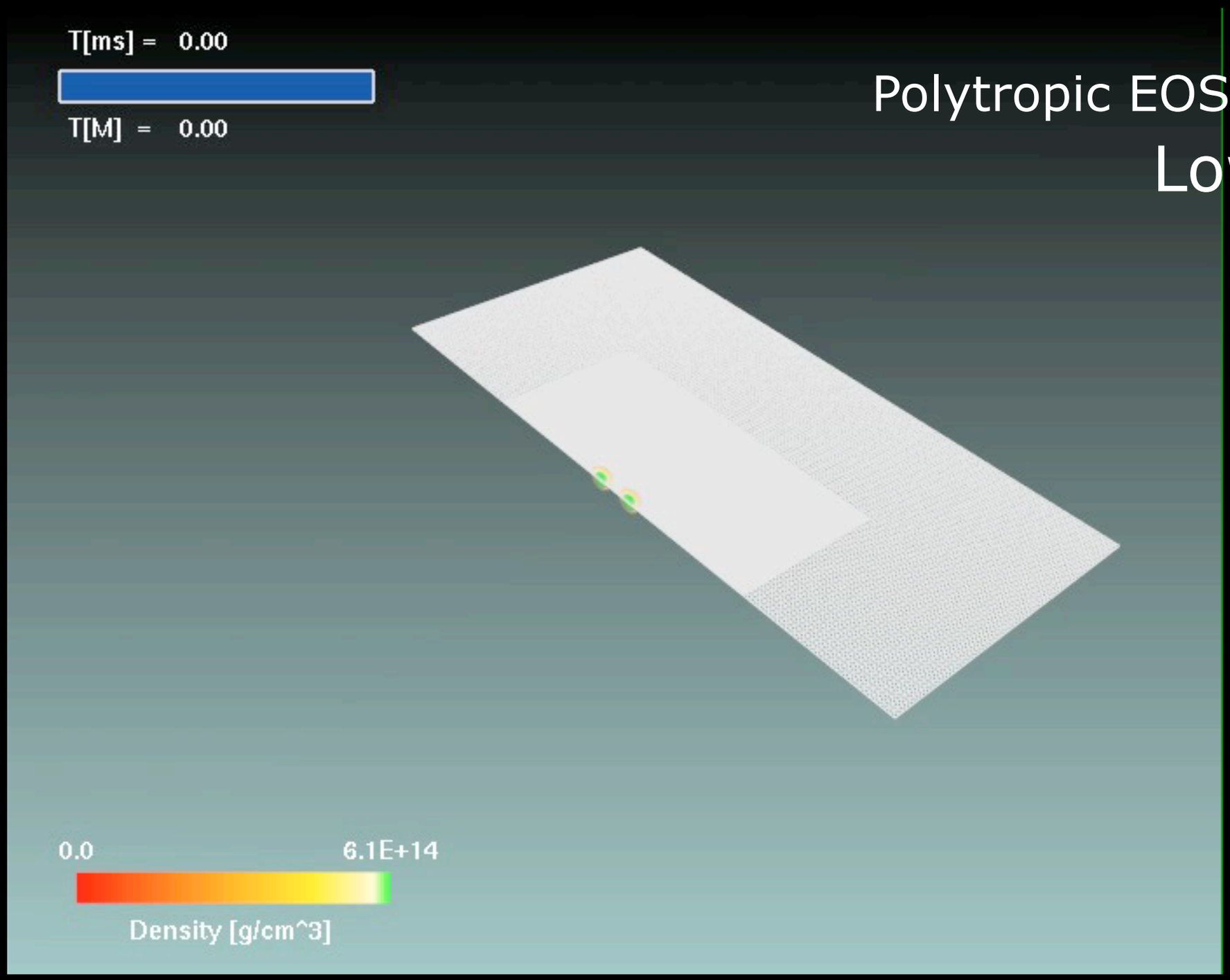

Polytropic EOS, 1.4 M_{sun}
Low mass

The HMNS is far from the instability threshold and survives for a longer time while losing energy and angular momentum.

After ~ 25 ms the HMNS has lost sufficient angular momentum and will collapse to a BH.

(Baiotti et al 2008)

Matter dynamics: effects of the total mass

high-mass binary

low-mass binary

(Baiotti et al 2008)

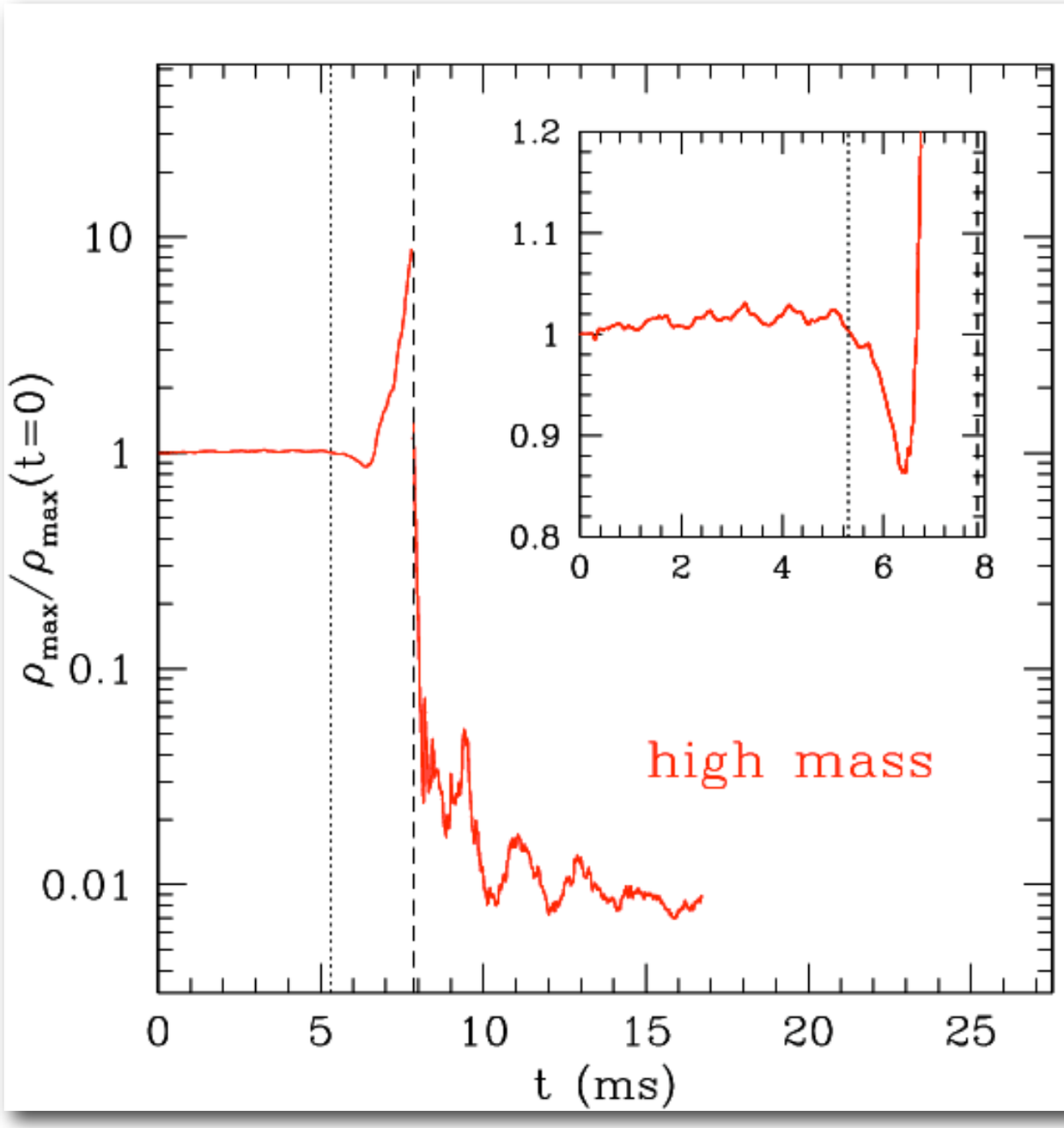

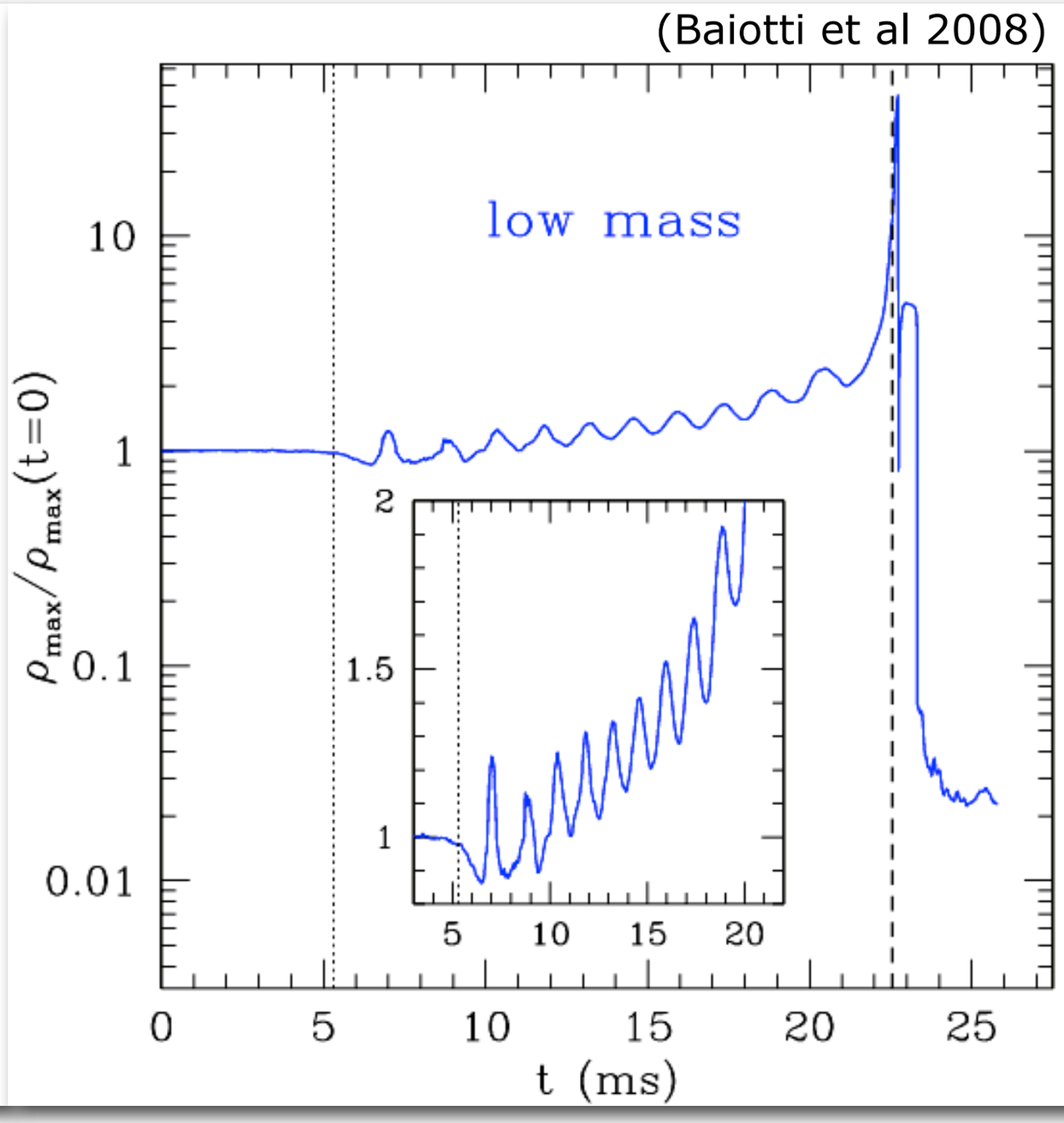

soon after the merge the torus is formed and undergoes oscillations

long after the merger a BH is formed surrounded by a torus

Gravitational waves from the BNS merger

Compact binary systems formed by two neutron stars, two black holes, or a mixed configuration, radiate a **burst of gravitational waves** during the catastrophic merger..

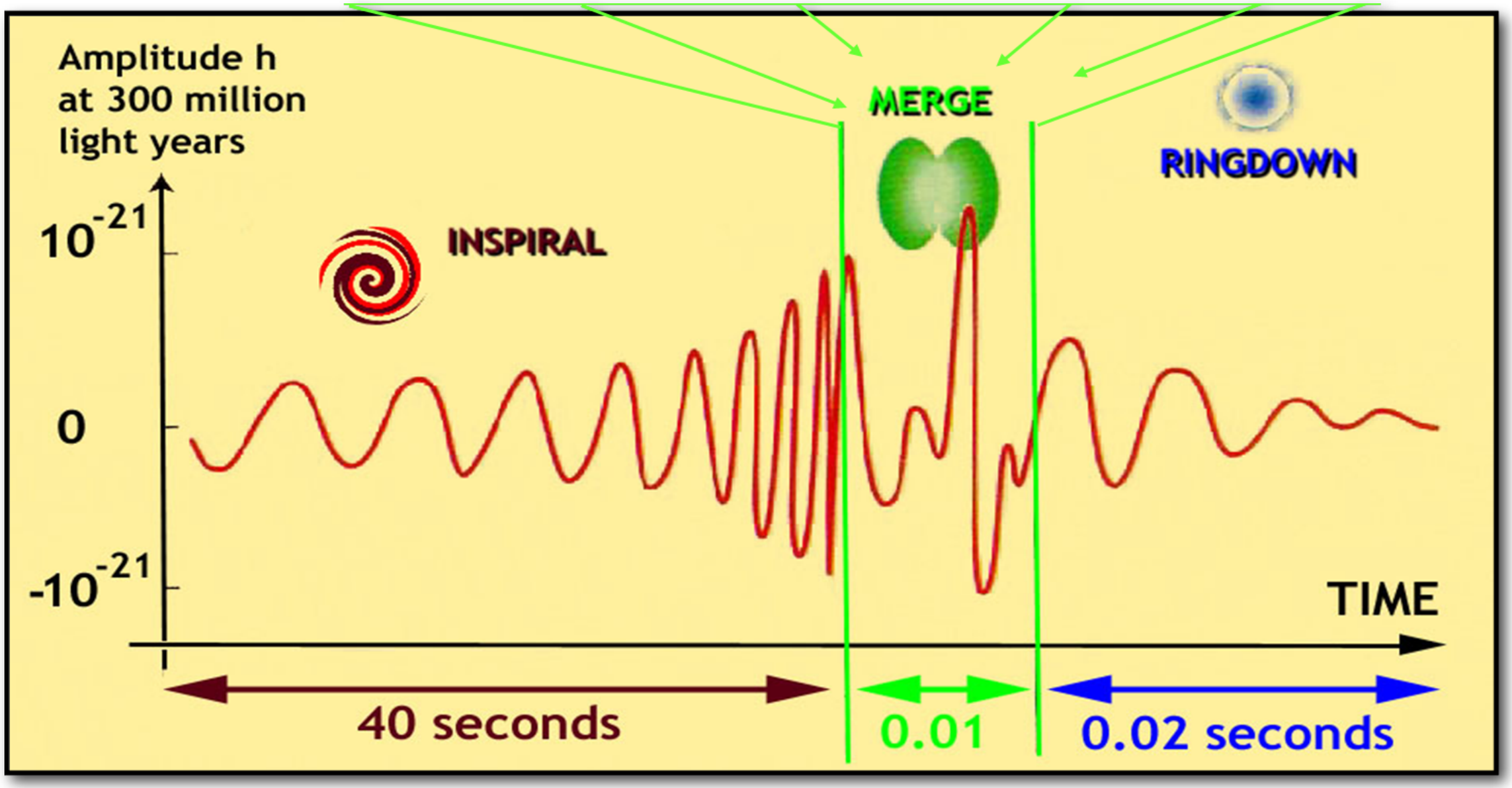

Gravitational wave extraction in (3+1) NR

First approach: perturbations on a Schwarzschild background expanding spatial metric into a tensor basis of Regge-Wheeler harmonics. Allows for extracting gauge-invariant wavefunctions given spherical surfaces of constant coordinate radius.

$$Q^{\times}_{lm} = \sqrt{\frac{2(l+2)!}{(l-2)!}}\left[c_1^{\times lm} + \frac{1}{2}\left(\partial_r - \frac{2}{r}c_2^{\times lm}\right)\right]\frac{S}{r}$$

$$Q^{+}_{lm} = \frac{1}{\Lambda}\sqrt{\frac{2(l-1)(l+2)}{l(l+1)}}(l(l+1)S(r^2\partial_r G^{+lm} - 2h_1^{+lm}) + 2rS(H_2^{+lm} - r\partial_r K^{+lm}) + \Lambda r K^{+lm})$$

These functions satisfy the Regge-Wheeler $(Q^{\times}_{lm})$ and Zerilli (Q^{+}_{lm}) wave eqs.

$$(\partial_t^2 - \partial_{r^*}^2)Q^{\times}_{lm} = -S\left[\frac{l(l+1)}{r^2} - \frac{6M}{r^3}\right]Q^{\times}_{lm}$$

$$(\partial_t^2 - \partial_{r^*}^2)Q^{+}_{lm} = -S\left[\frac{1}{\Lambda^2}\left(\frac{72M^3}{r^5} - \frac{12M(l-1)(l+2)}{r^3}\left(1 - \frac{3M}{r}\right)\right) + \frac{l(l^2-1)(l+2)}{r^2\Lambda}\right]Q^{+}_{lm}$$

with the definitions: $S = 1 - \frac{2M}{r}$ $\Lambda = (l-1)(l+2) + \frac{6M}{r}$

$$r^* = r + 2M\ln(r/2M - 1)$$

Gravitational wave extraction in (3+1) NR

At a sufficiently large distance from the source and assuming the spacetime resembles that of a Schwarzschild black hole, the gravitational waves in the two polarizations can be written in terms of the odd and even-parity gauge invariant perturbations of a Schwarzschild black hole as

$$h = h_+ - i h_\times = \frac{1}{\sqrt{2}r} \sum_{l,m} \left(Q^+_{lm} - i \int_{-\infty}^{t} Q^\times_{lm}(t'\, dt') \right) Y^{-2}_{lm} + \mathcal{O}\left(\frac{1}{r^2}\right)$$

Second approach: projection of the Weyl tensor onto components of a null tetrad.

At a sufficiently large distance from the source and in a Newman-Penrose tetrad frame, the gravitational waves in the two polarizations can be written in terms of the Weyl scalar Ψ_4 as

$$h = h_+ - i h_\times = - \int_{-\infty}^{t} dt' \int_{-\infty}^{-t'} \Psi_4 \, dt''$$

The Weyl scalar Ψ_4 can be computed explicitly in terms of projections of the 4-Riemann tensor onto a null Newman-Penrose tetrad.

Gravitational radiation from *the* merger

Dynamics

Signal amplitude

(AEI)

Gravitational radiation from *the* merger

Dynamics

Signal amplitude

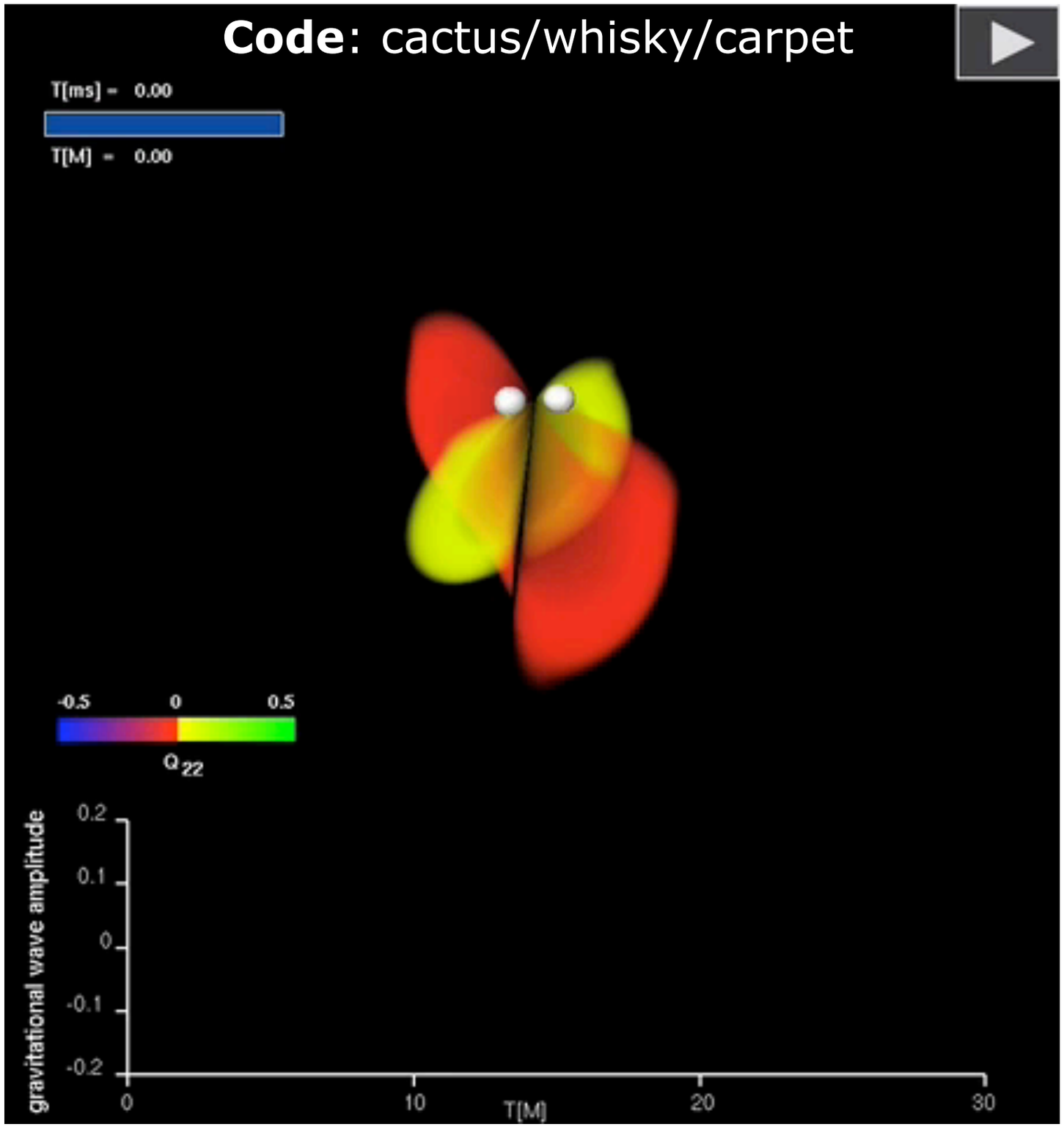

(AEI)

Waveforms: strong dependence on total mass

(Baiotti et al 2008)

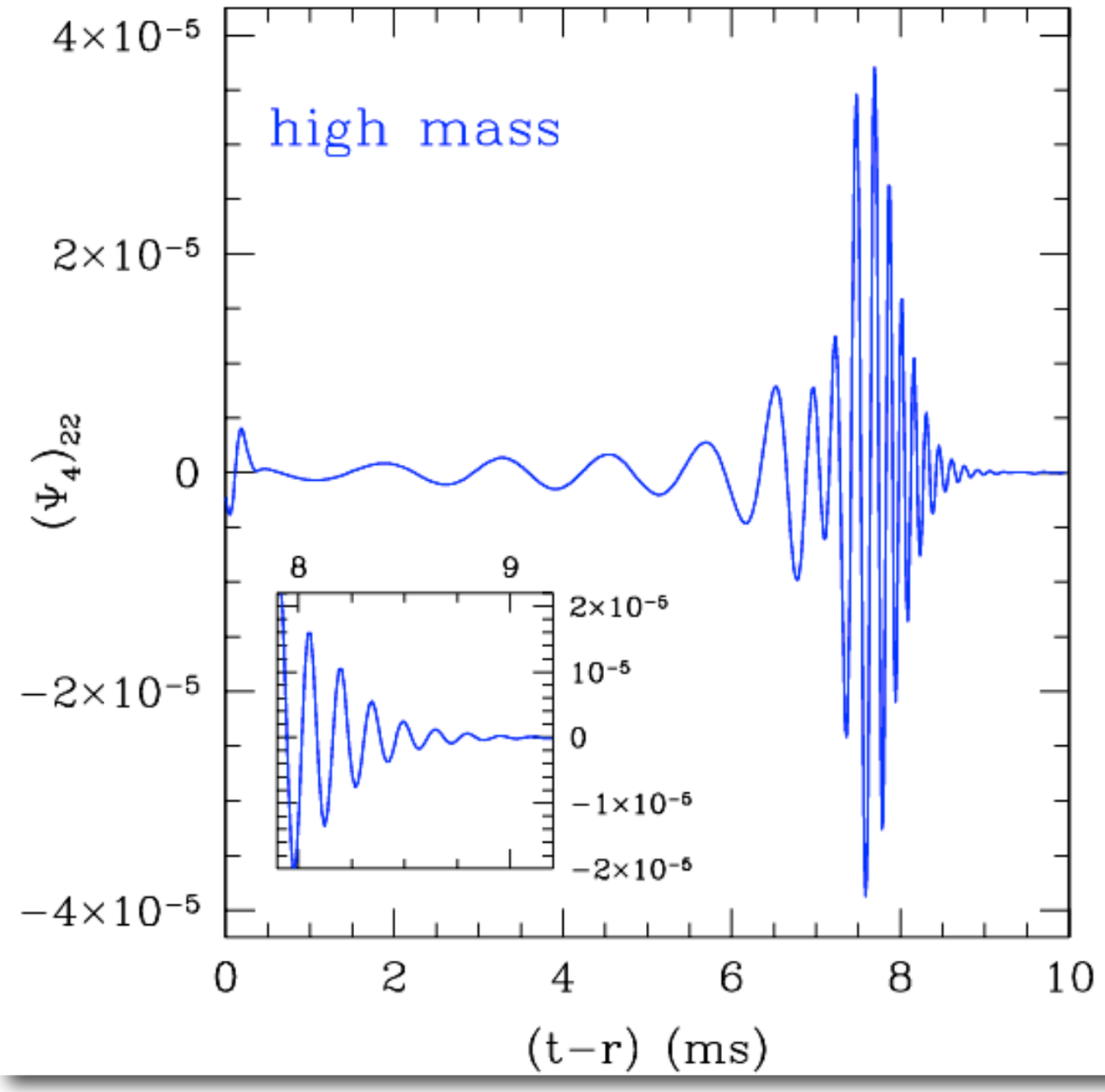

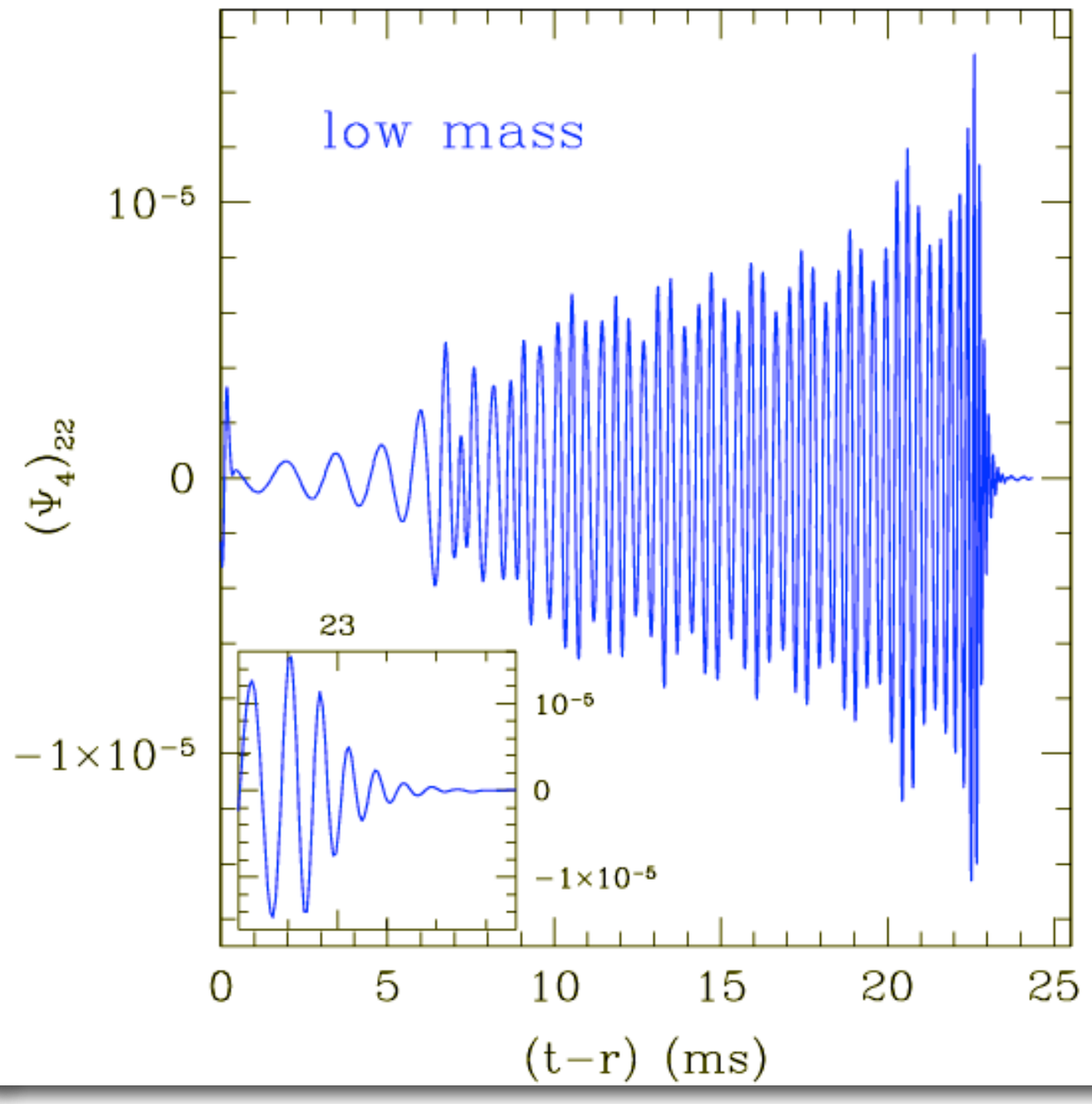

Small variations in the total mass of the initial models yield important differences in the gravitational waveforms

Imprint of the EOS: ideal fluid vs polytropic

(Baiotti et al 2008)

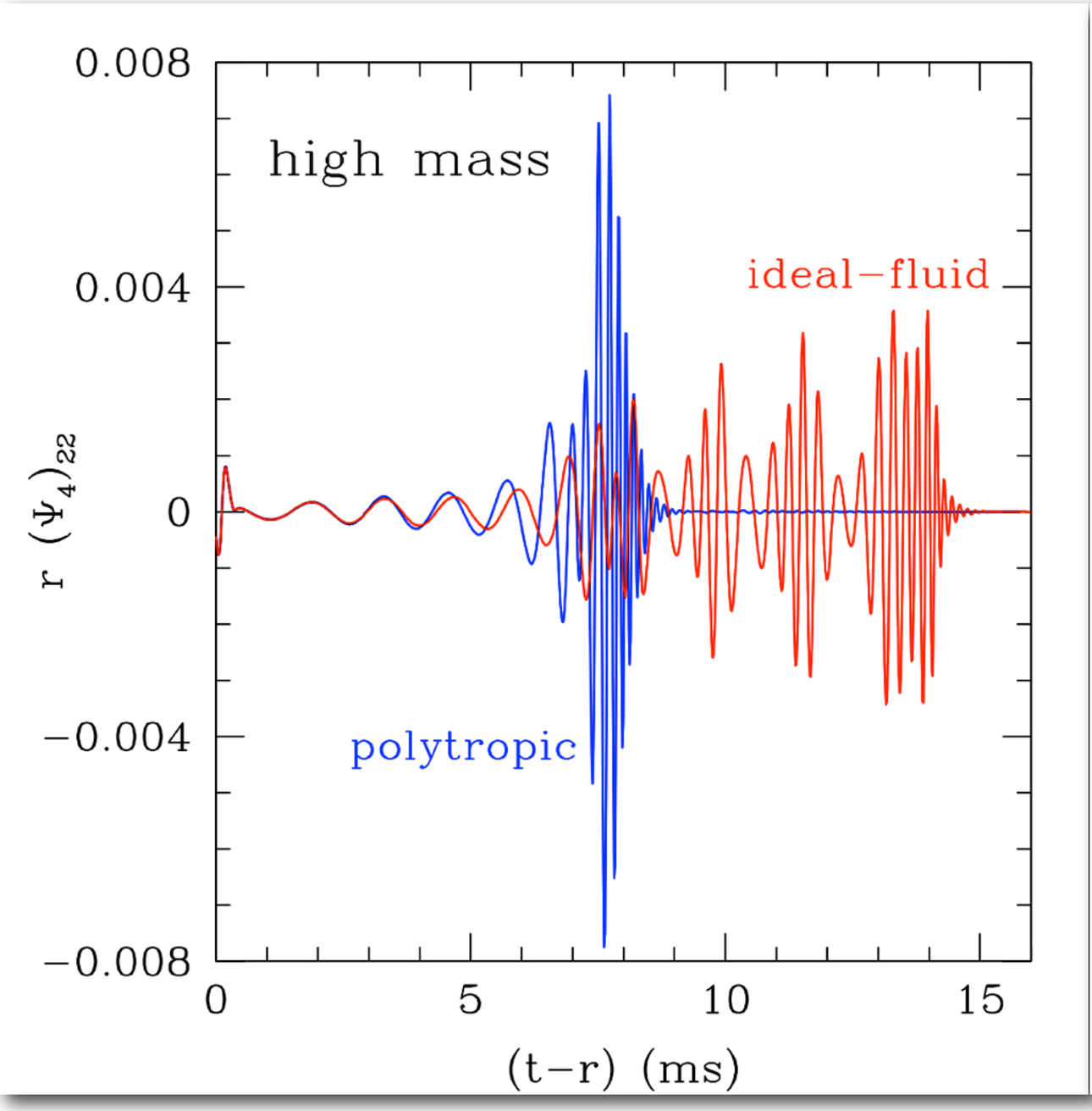

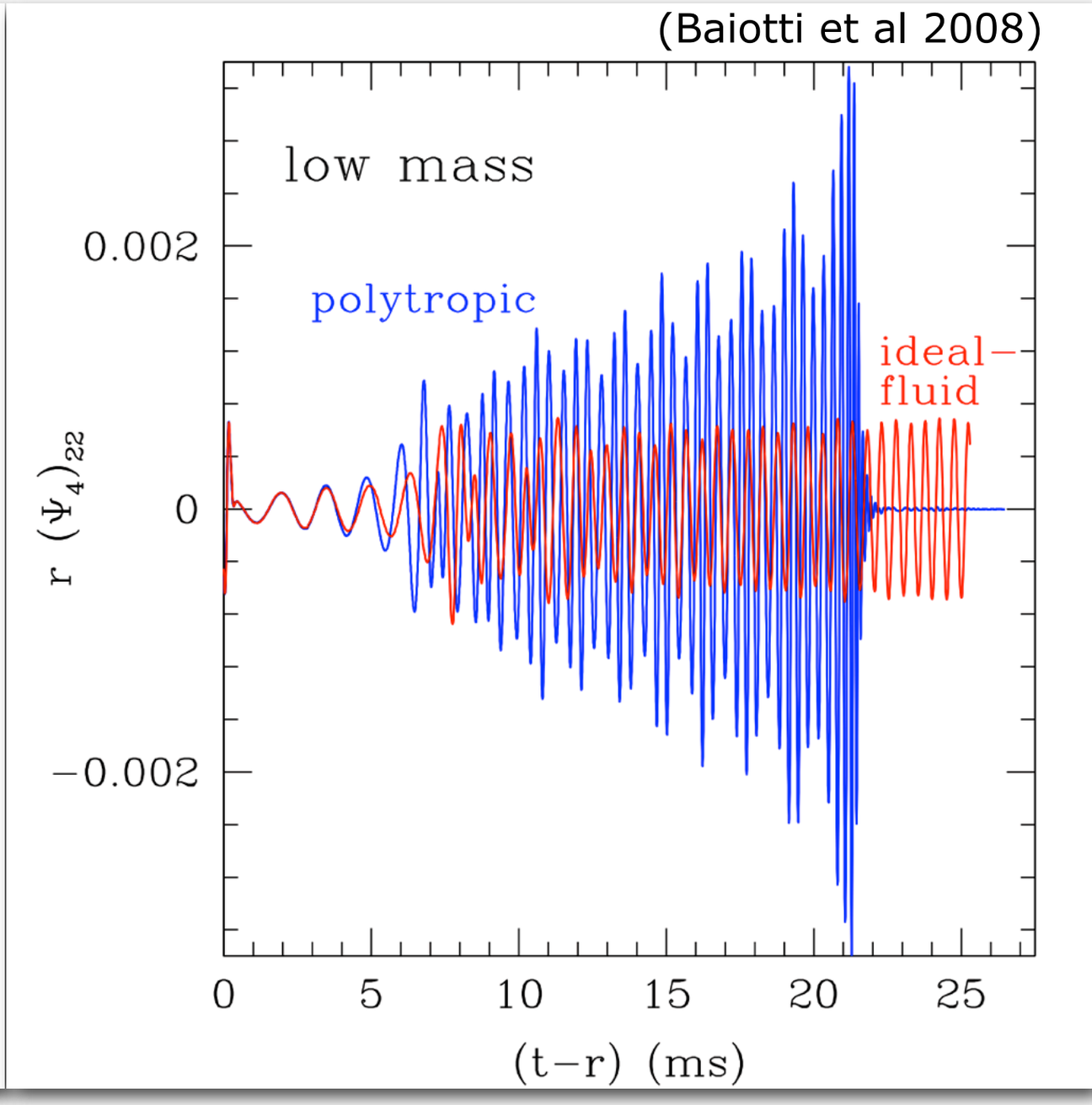

After the merger a BH is produced over a timescale comparable with the dynamical one

After the merger a BH is produced over a timescale larger or much larger than the dynamical one

Unequal-mass BNS merger

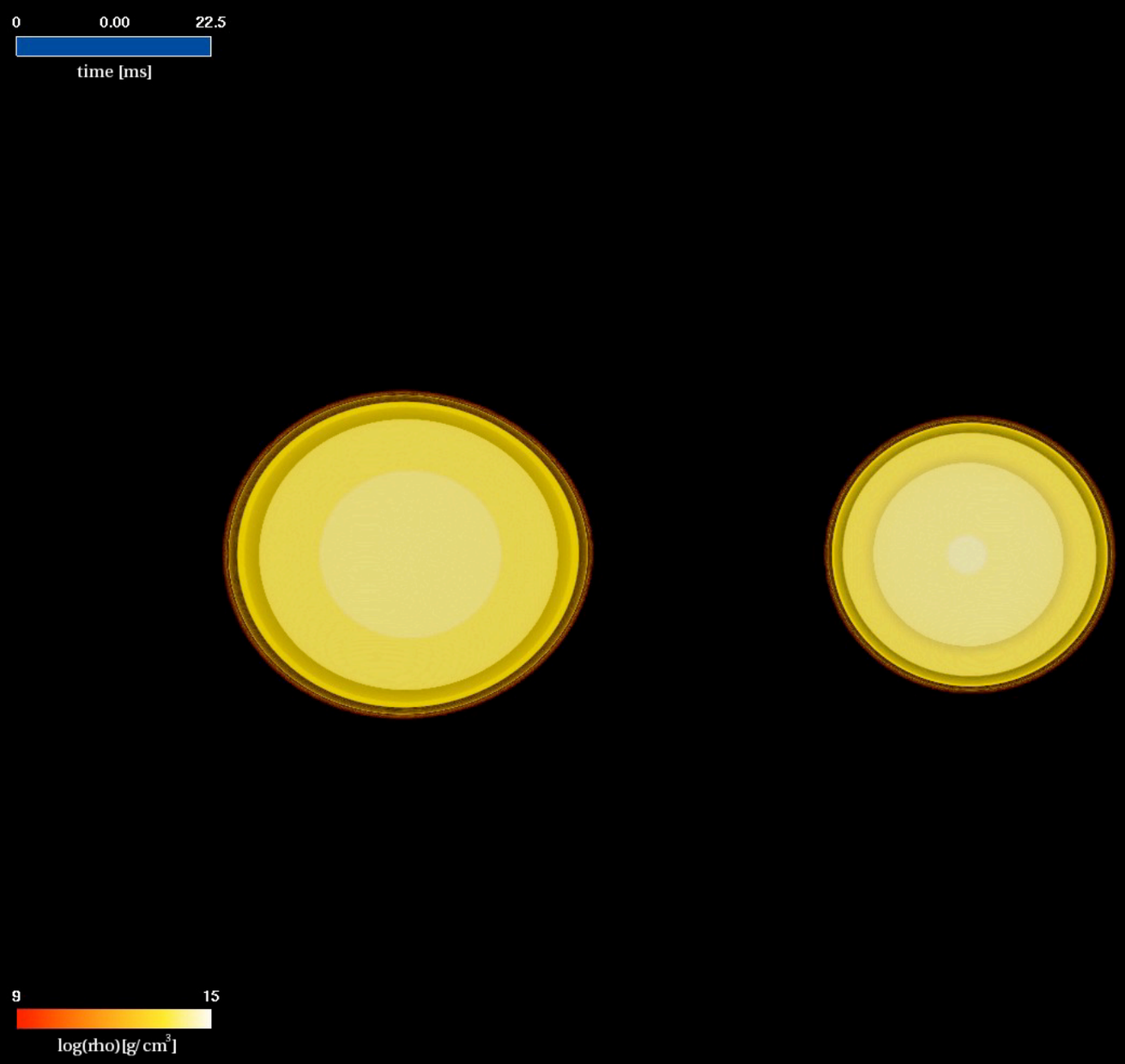

A significantly more massive torus is formed in this case.

(Rezzolla et al 2010)

Morphological differences (at onset of QSA)

q=1.0

q=0.7

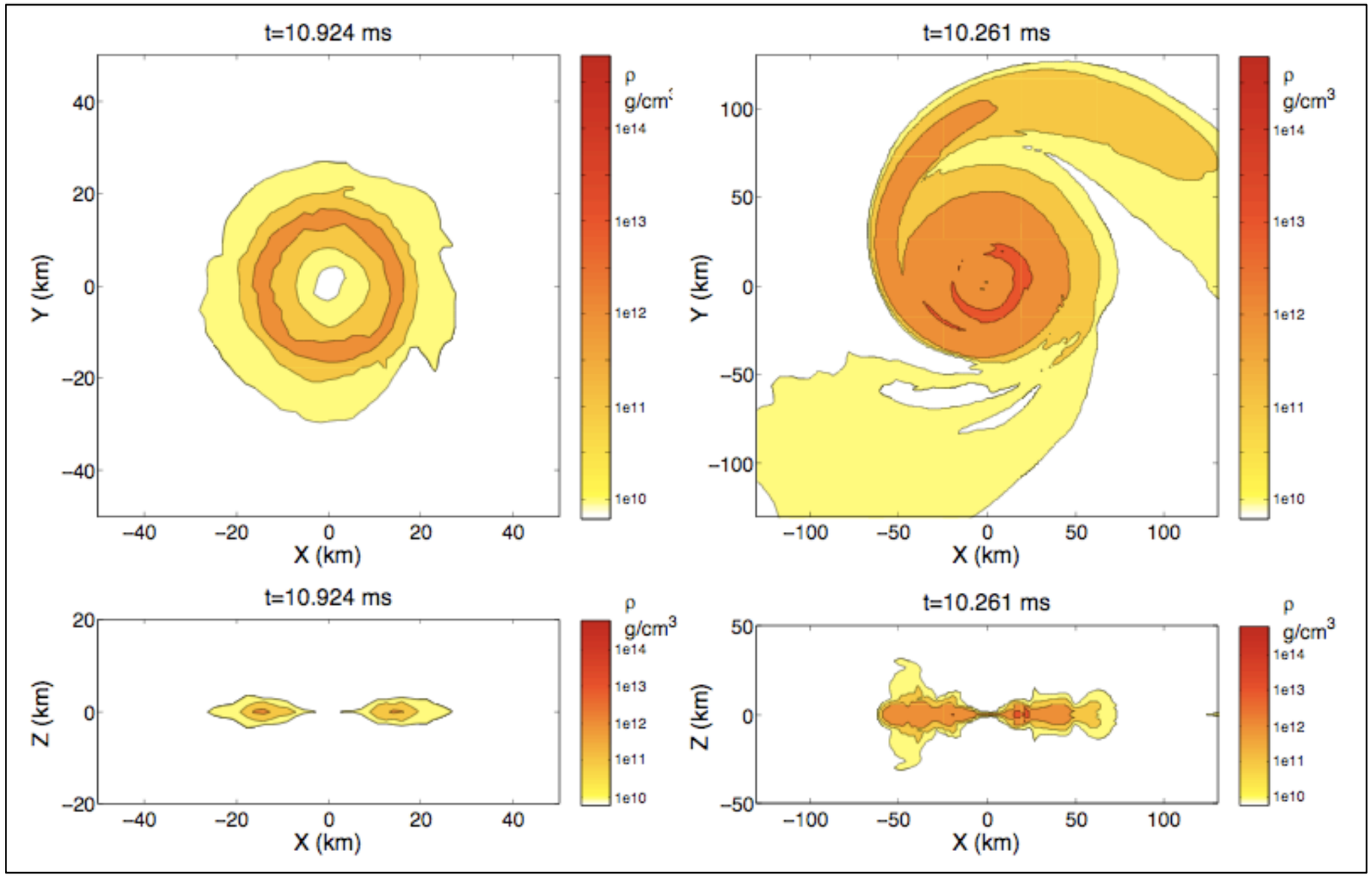

Highly symmetric disk.
Geometrically thin.

Large asymmetry, spiral arm not yet accumulated onto central disk surrounding BH.

Morphological differences (at end of simulation)

q=1.0 q=0.7

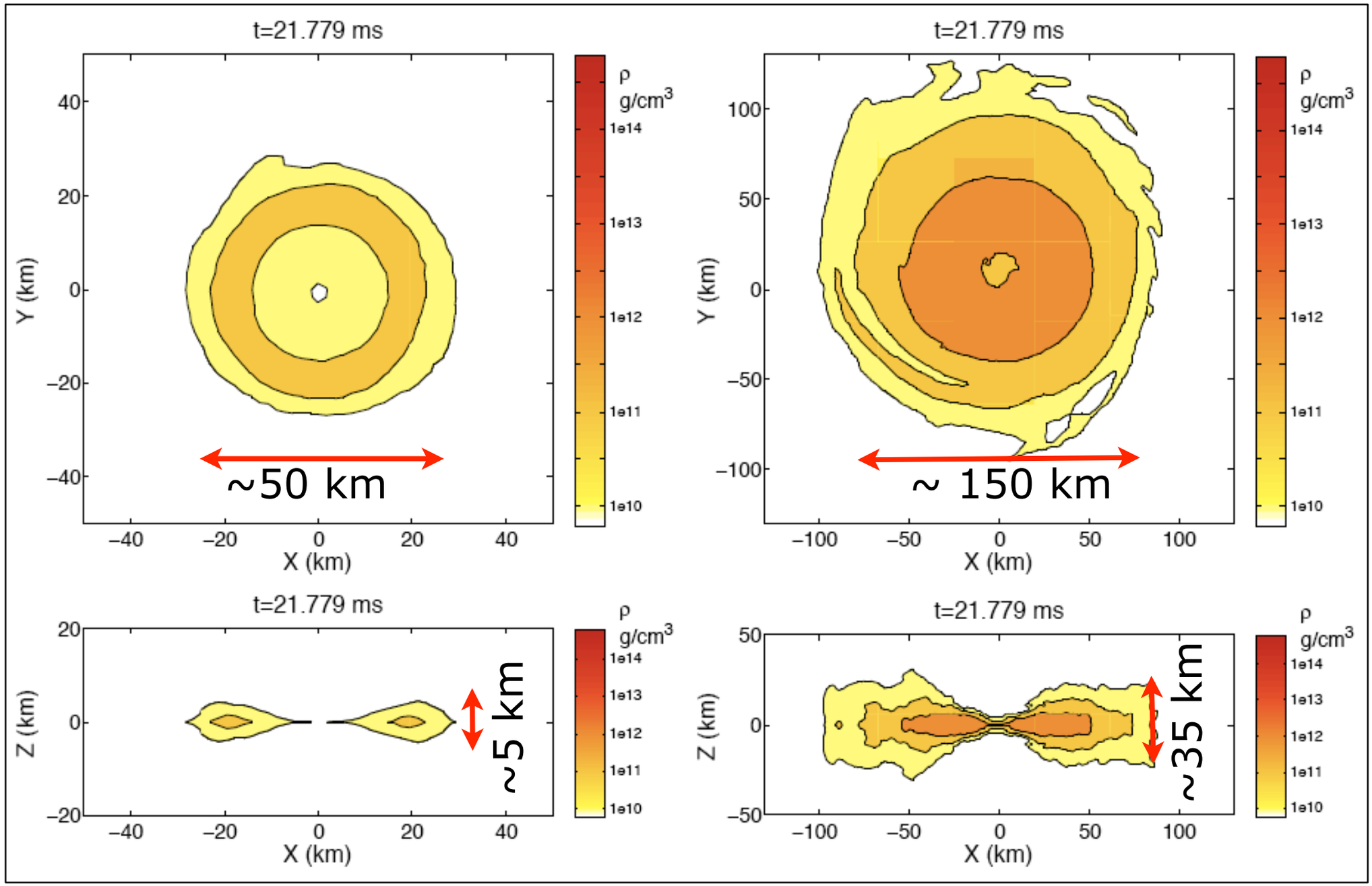

Symmetric. Thin disk. Axisymmetric shape. Thick disk.

Both tori differ in size by about a factor ~3 and in mass by about a factor ~200. However, they have comparable mean rest-mass densities.

Evolution of total rest mass

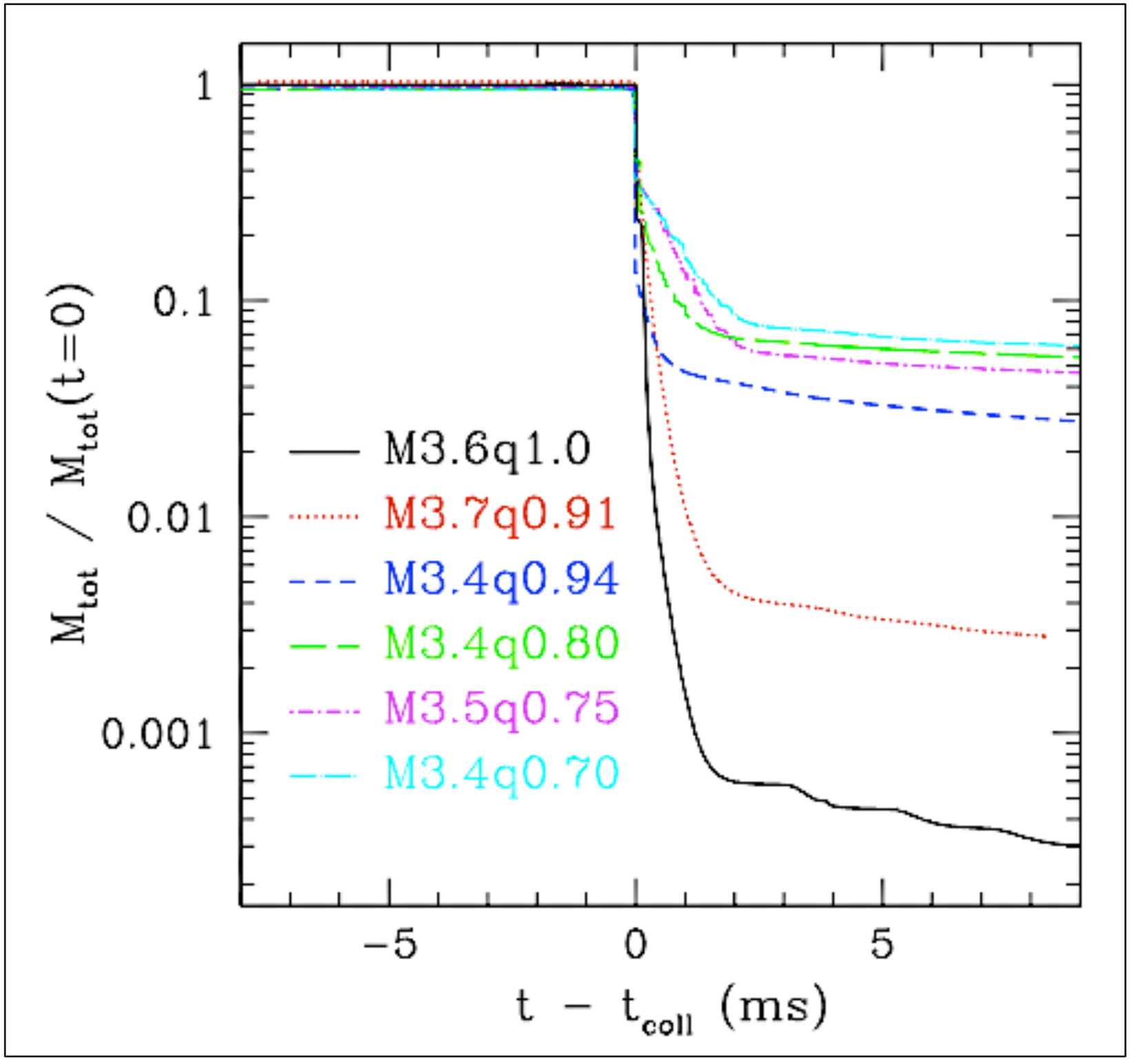

Curves shifted in time to coincide at collapse time.

Mass of resulting disk is larger for smaller values of *q*.

Trend not entirely monotone as it is also influenced by the initial total baryonic mass of binary.

Model
M3.6q1.00
M3.7q0.94
M3.4q0.91
M3.4q0.80
M3.5q0.75
M3.4q0.70

Evolution of total mass and accretion rate

The **torus mass** is defined as the total rest mass outside the AH when the disk enters a regime of quasi-steady accretion **(QSA)**. The onset of the QSA is defined as the point in time when the condition mass flux / total mass < $10^{-6}(Gc^{-3}M_{\odot})^{-2}$ is satisfied for the first time.

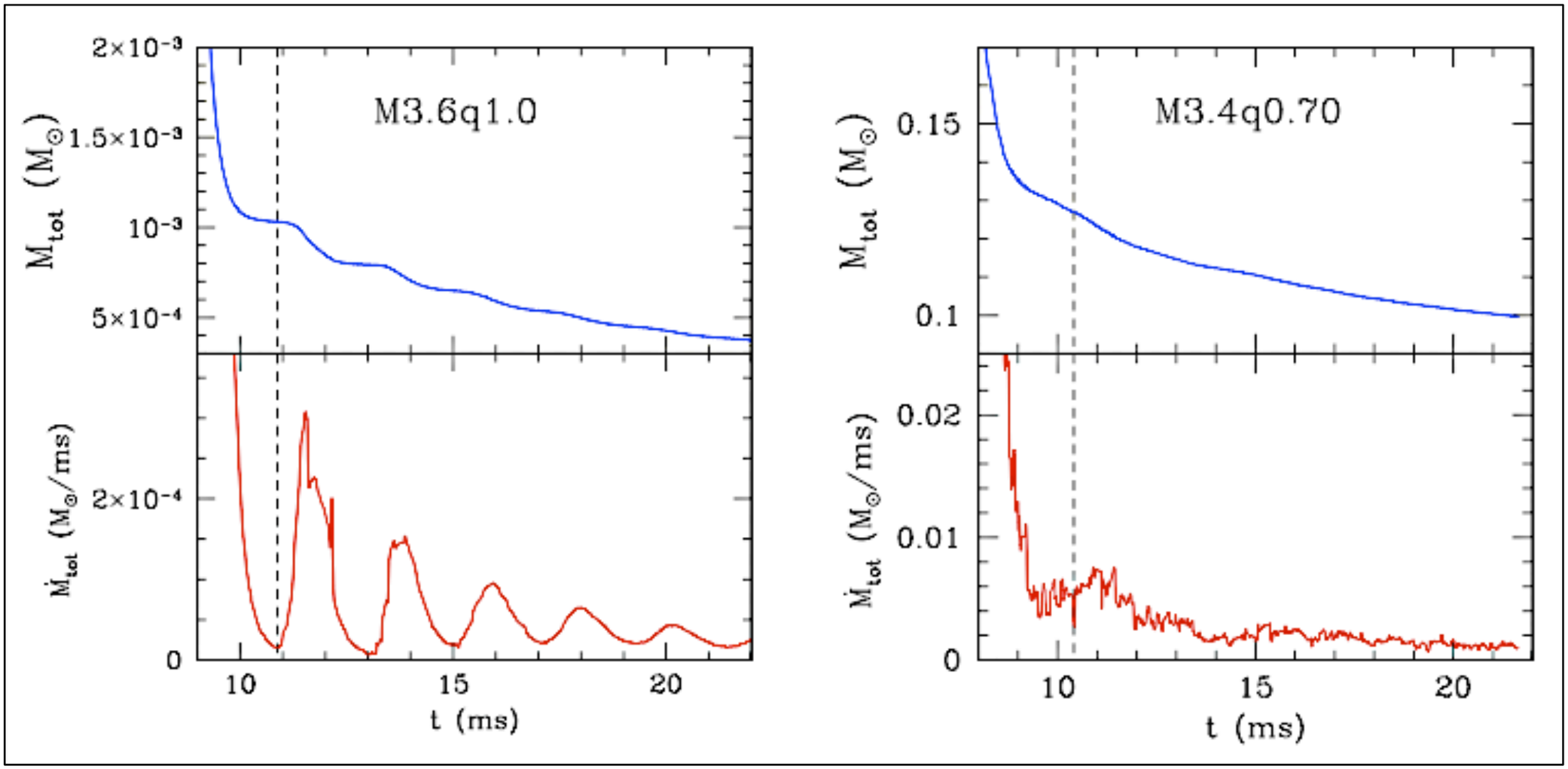

Equal-mass model shows an accretion rate that is subject to **quasi-periodic oscillations** as the torus moves in and out at about the radial epicyclic frequency.

The mass flux of the **unequal-mass model** is rather **constant in time** and this reflects a very different distribution of angular momentum in the tori.

Evolution of rest-mass density

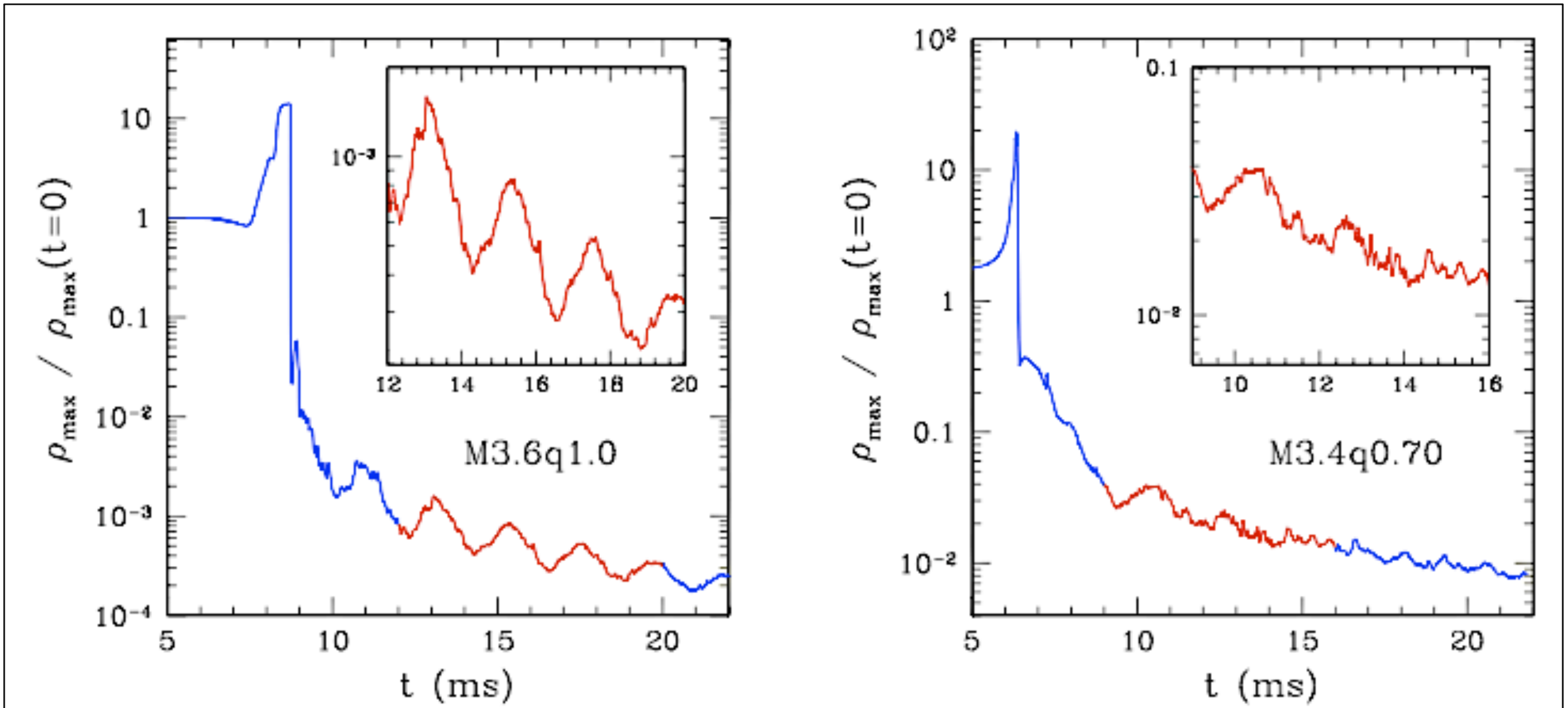

Harmonic behaviour also apparent in the evolution of the maximum of the rest-mass density.

Oscillating tori as gravitational wave source

General relativistic hydrodynamical (and MHD) “test-fluid” simulations have shown that high density relativistic tori (around Schwarzschild or Kerr black holes) and subject to perturbations, undergo a persistent oscillation phase and are a promising new source of GWs.

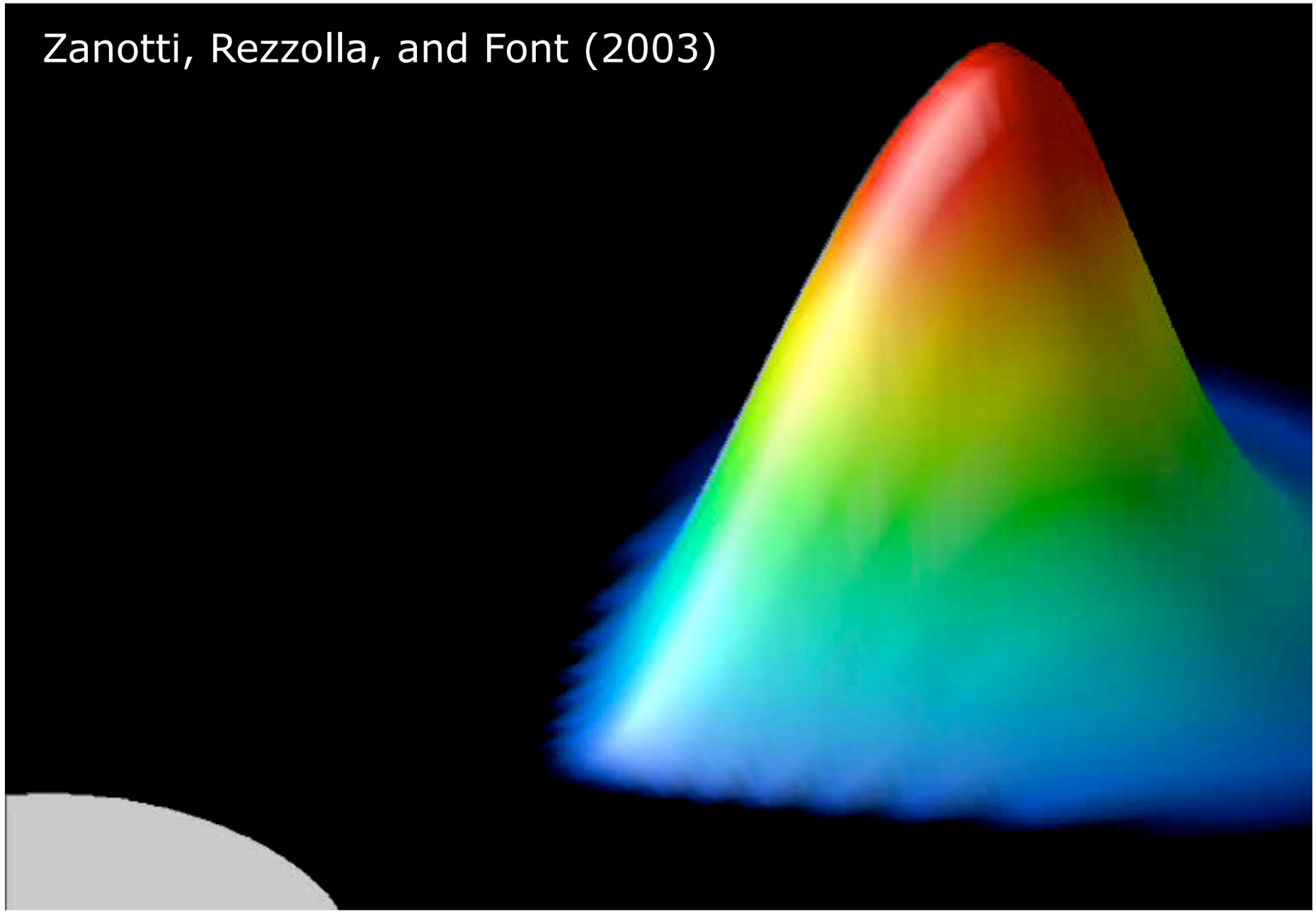

Oscillating tori as gravitational wave source

Time evolution of mass quadrupole

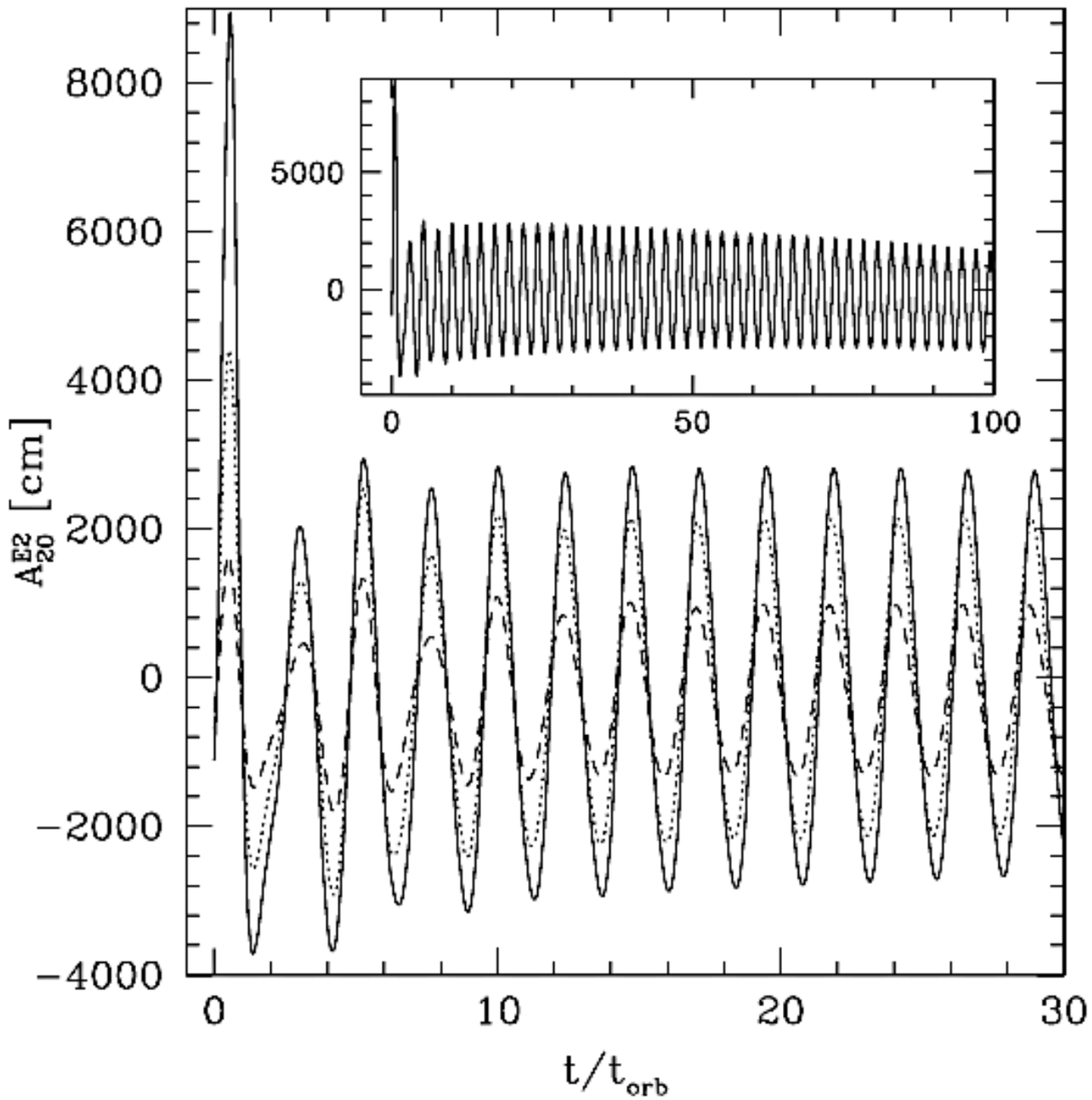

Gravitational wave amplitude

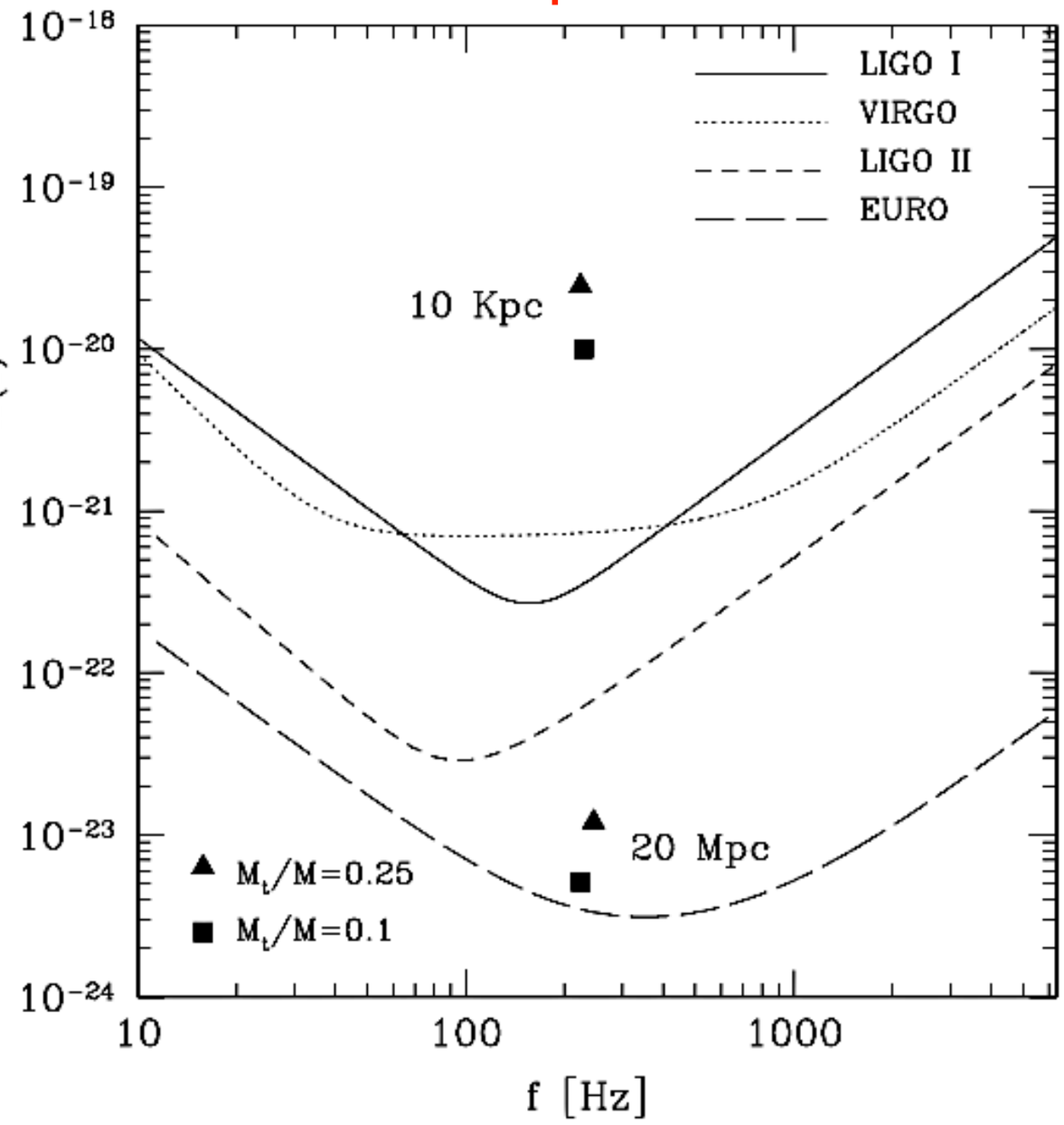

Zanotti, Rezzolla, and Font (2003)

p-mode oscillations of relativistic tori **(test fluid)**

Our self-consistent simulations lead to disks showing harmonic behaviour in the accretion process.

The dynamics of oscillating relativistic tori in equilibrium analyzed extensively (Rezzolla et al 2003; Zanotti et al 2003, 2005; Montero et al 2007) in the test-fluid approximation, with and without magnetic fields, and for the cases of Schwarzschild and Kerr BHs.

Upon the introduction of perturbations in the tori, a long-term oscillatory behavior is found, lasting for tens of orbital periods.

These oscillations correspond to axisymmetric **p-mode oscillations** whose lowest-order frequencies appear in the **harmonic sequence 2:3.**

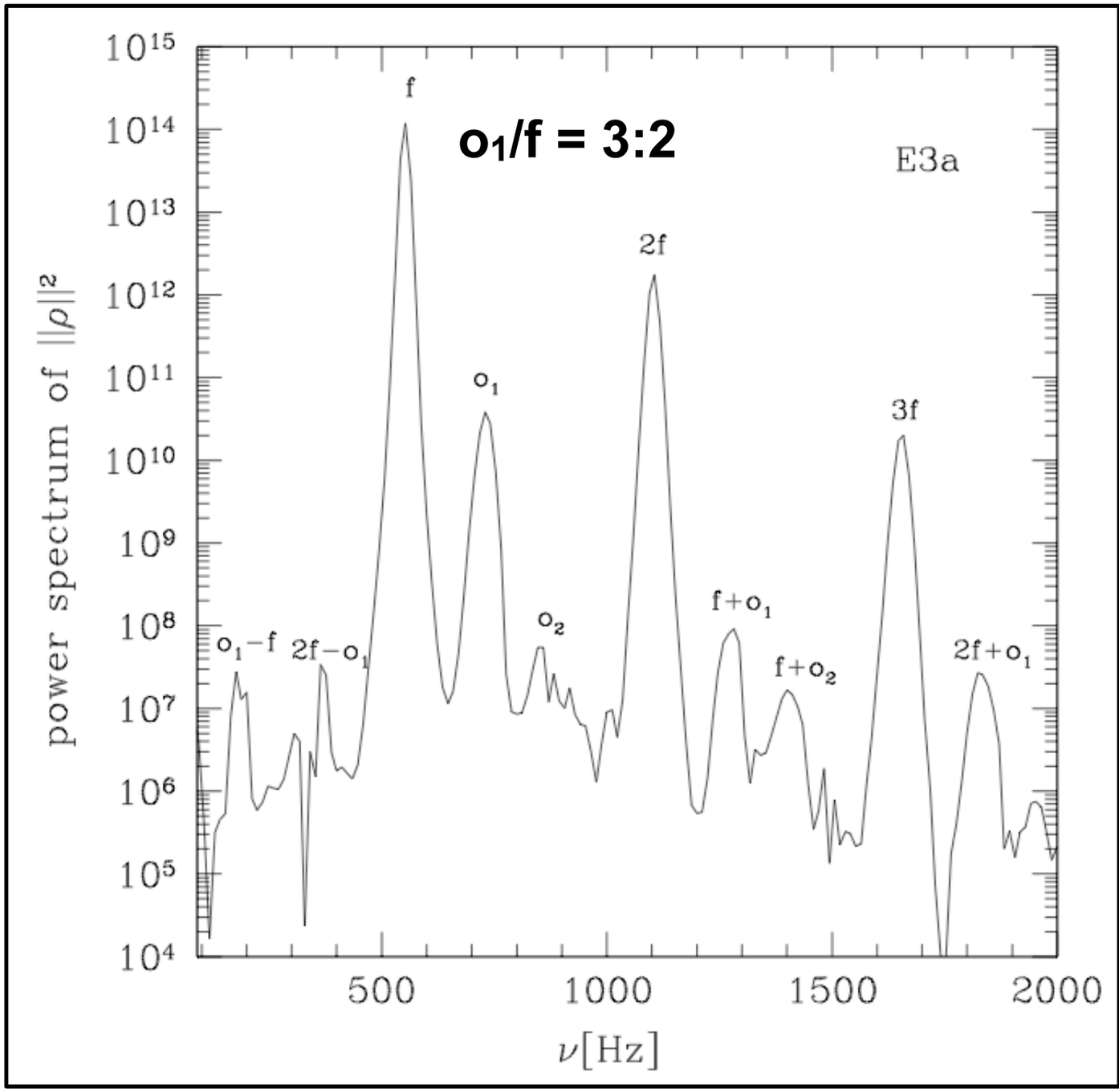

Zanotti, Font, Rezzolla & Montero (2005)

p-mode oscillations of **self-gravitating** tori

Those studies have been extended by Montero, Font & Shibata (2010), where systems formed by a BH (in the puncture framework) surrounded by (marginally stable) **self-gravitating disks** were evolved in axisymmetry. Even in this case, the ratio of the fundamental oscillatory mode and the first overtone also shows approximately the **2:3 harmonic relation** found in earlier works.

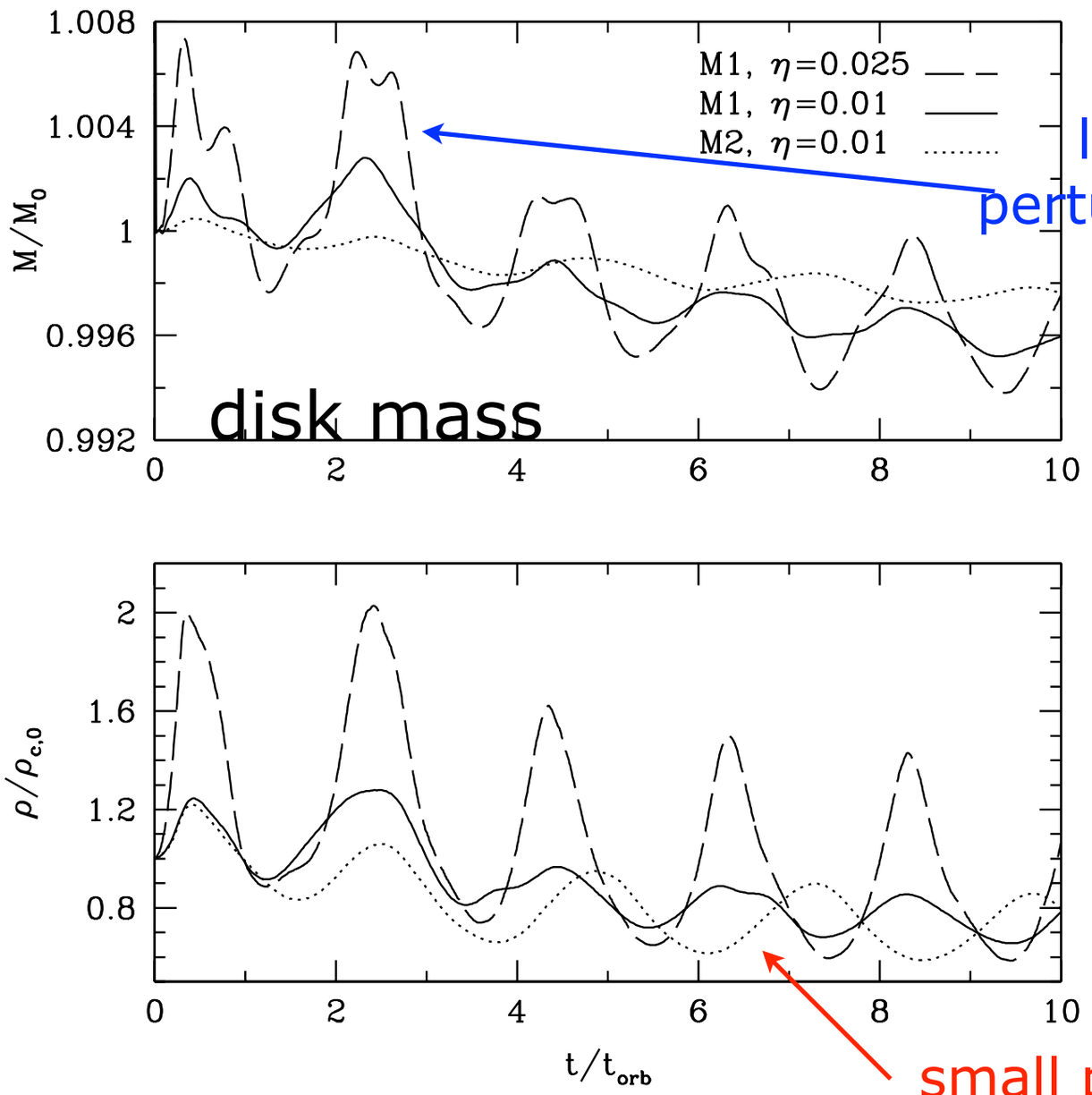

p-mode oscillations of **tori from BNS mergers**

The dynamics of the BH–torus system produced by the merger of model M3.6q1.00 is more complicated than that considered in the test-fluid studies, for which initial configurations in stable equilibrium exist.

Our systems studied *ab-initio* as the end-products of highly dynamical events, yet so much of the phenomenology found in previous works also applies here.

Timeseries too short to provide firm evidence of the 2:3 harmonic relation. Spectral analysis **excess power present at such frequencies.**

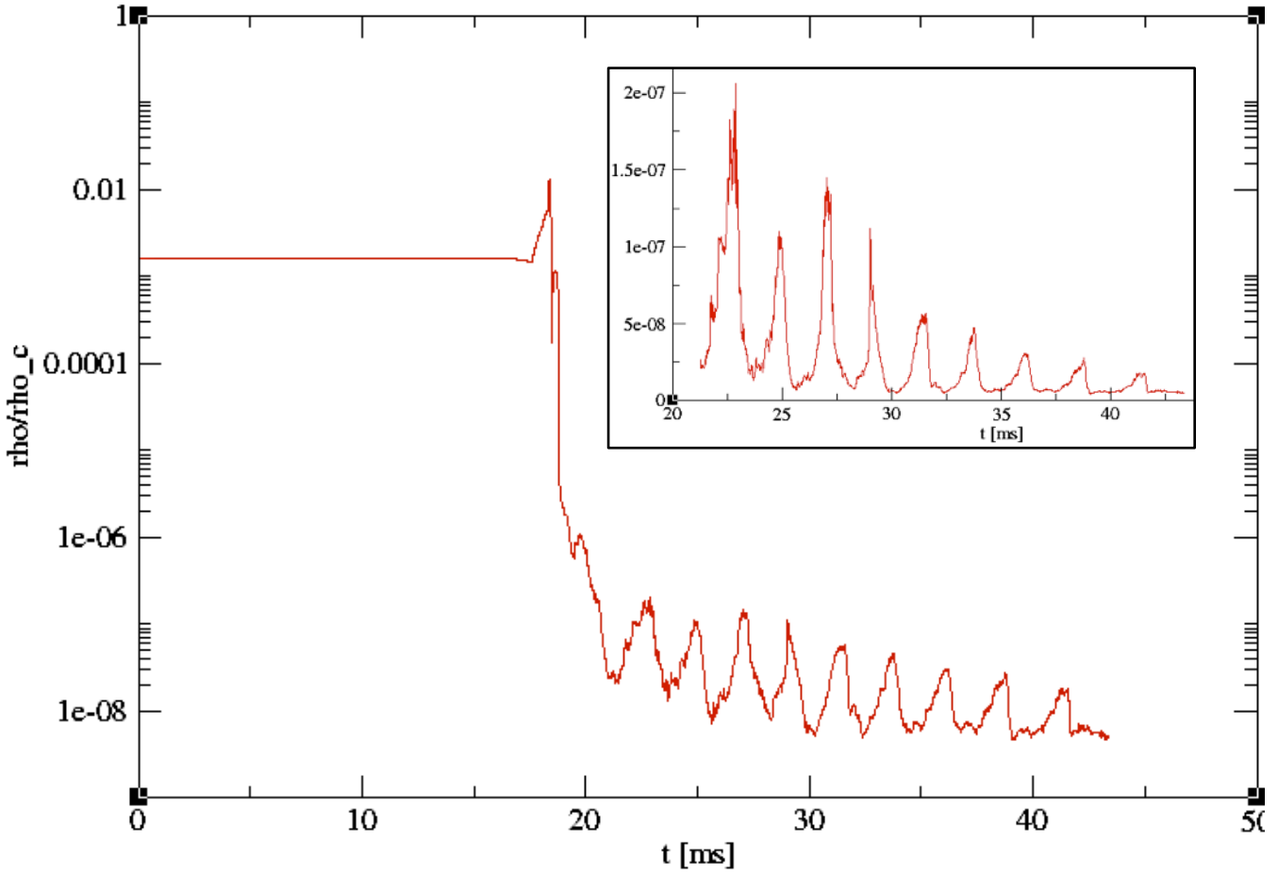

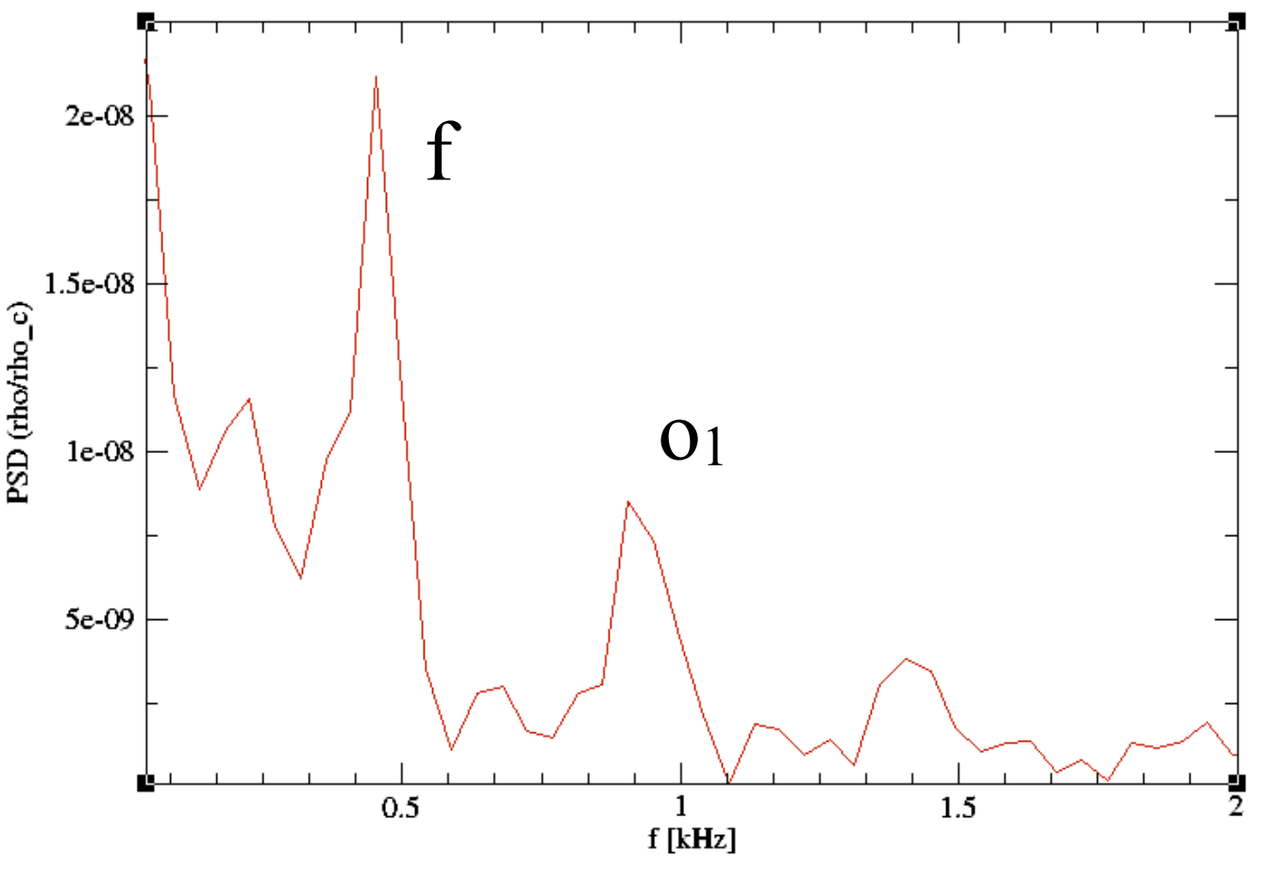

Black hole + accretion torus system

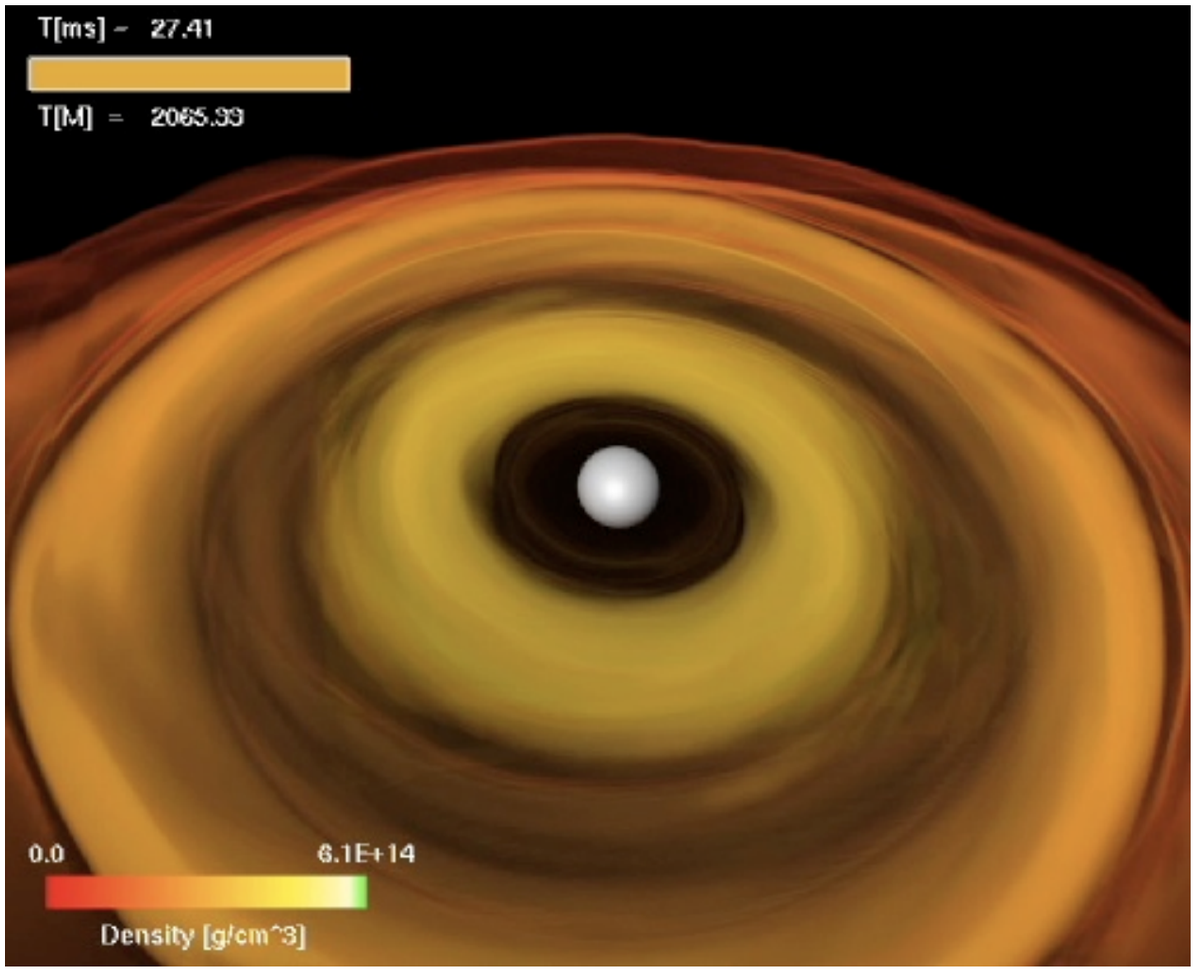

Numerical simulations of NS-NS show that most of the material disappears beyond the event horizon in a few ms.

As a result, a thick accreting disk or torus with mass of about 10% of total mass (upper limit) may be formed.

The formation and evolution of BH-torus systems have not yet been observed as such sites are opaque to electromagnetic waves (EWs) due to their intrinsic high density and temperature.

Gravitational waves (GWs) are much more transparent than EWs with respect to absorption and scattering with matter.

If BH-torus systems emitted detectable GWs, it would be possible to explore their formation and evolution, along with the prevailing hypotheses that associate them to GRB engines.

Gamma-ray burst mechanism in a nutshell

In a GRB the energy supply comes from the energy released by the accretion of disk material onto the BH and from the rotational energy of the BH itself, which can be extracted, for instance, via the Blandford-Znajek mechanism.

This vast amount of energy (of the order of 10^{53}–10^{54} erg, depending on the mass of the disk and on the BH rotation and mass) is sufficient to power a GRB if the energy released can be converted into gamma-rays with an efficiency of about a few percent.

This scenario requires a **stable enough system to survive for a few seconds.** In particular, the internal-shock model (Rees & Meszaros 1994) implies that the duration of the energy release by the source has a duration comparable with the observed duration of the GRB.

Any instability which might disrupt the system on shorter timescales, such as the so-called runaway instability and the Papaloizou-Pringle instability, could pose a severe problem for the accepted GRB models.

The runaway instability (I)

In a black hole + thick disk system the gas flows in an effective (gravitational + centrifugal) potential whose structure is similar to that of a close binary. The Roche torus has a cusp-like inner edge at the Lagrange point L1 where mass transfer driven by the radial pressure gradient is possible.

These systems may be subjected to a **runaway instability** (Abramowicz et al 1983): due to accretion from the disk the BH mass and spin increase and the gravitational field changes. Two evolutions feasible to reach new equilibrium solution:

1. Cusp moves inwards toward the BH, mass transfer slows down. **Stable**.
2. Cusp moves deeper inside the disc material, mass transfer speeds up. **Unstable**.

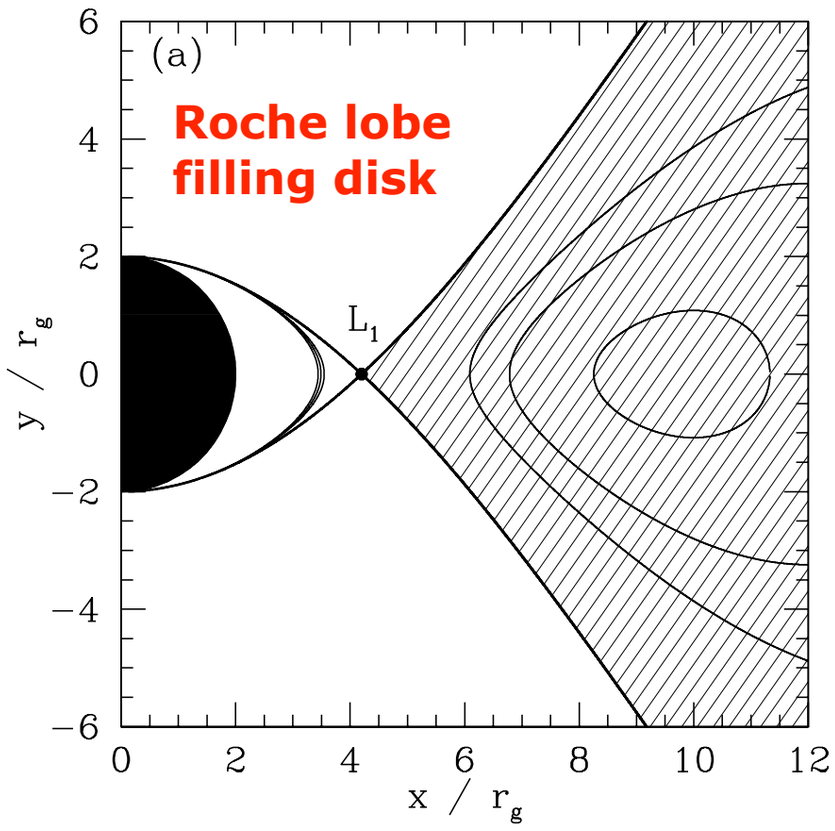

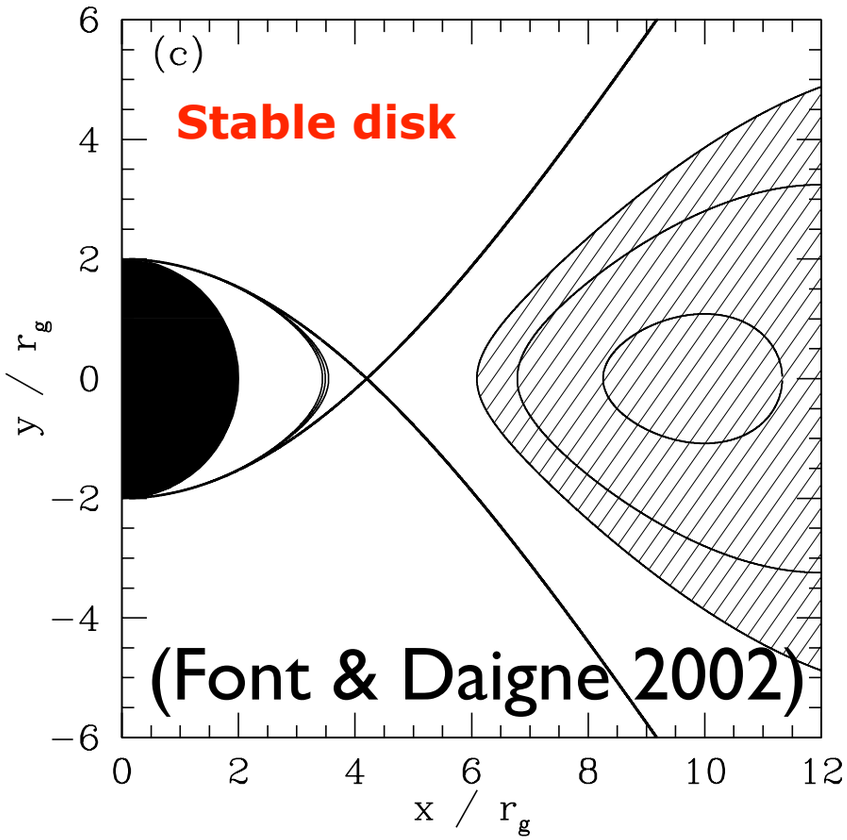

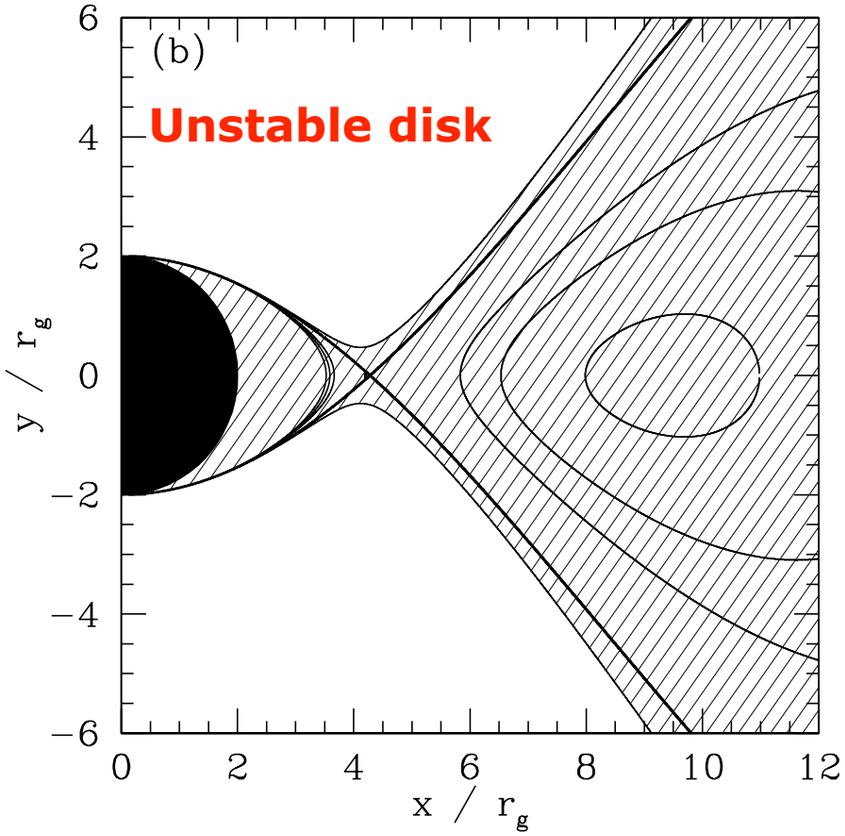

The runaway instability (II)

Recent numerical relativity simulations have shown that the runaway instability does not have a significant impact on the dynamics even if the torus self-gravity is taken into account.

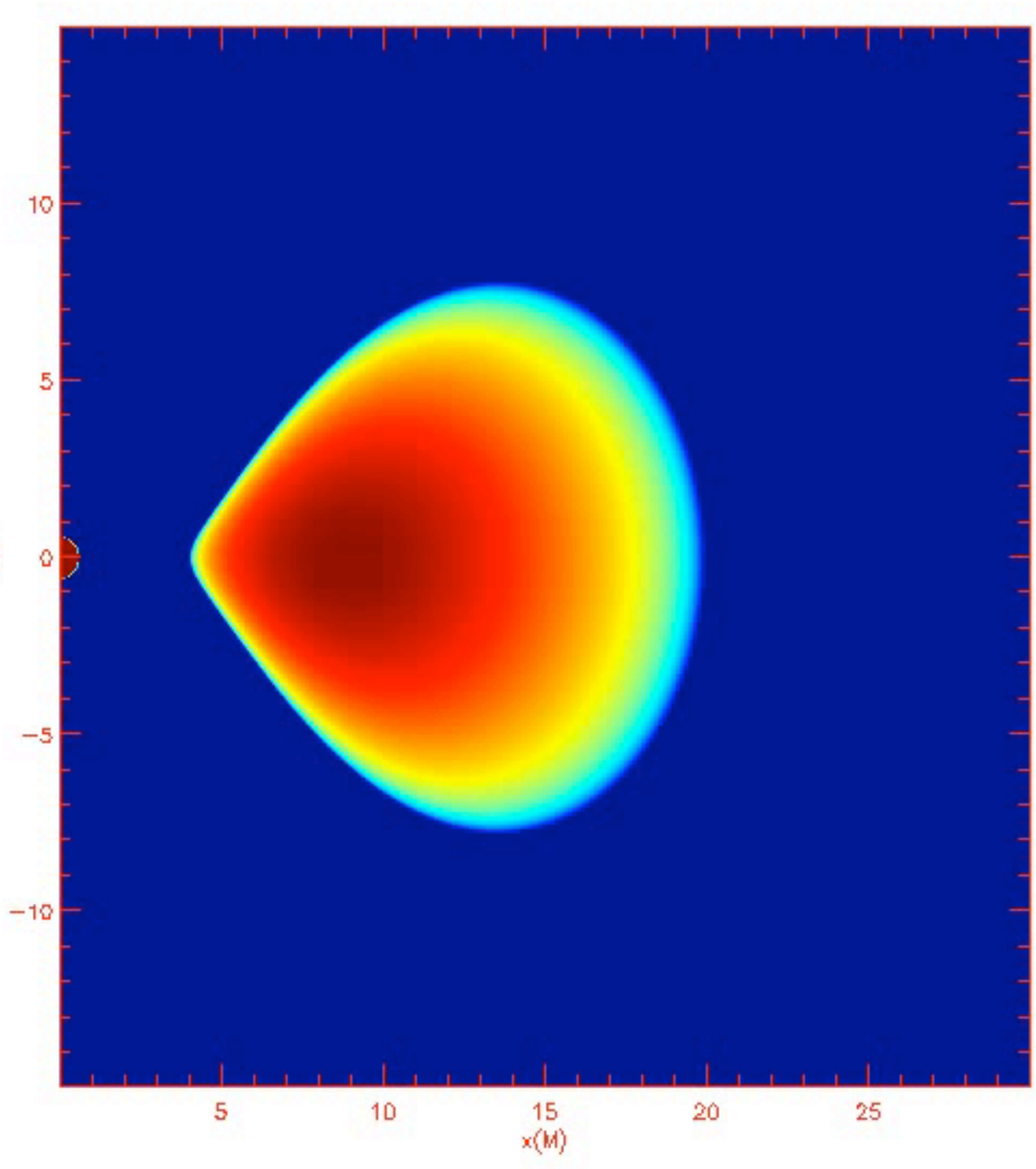

Self-gravitating torus in equilibrium around a black hole ($M_t/M_{BH}=1$).

Axisymmetric simulation (2D).

An initial perturbation induces the transfer of small amount of matter through the cusp towards the BH.

This does not reduce significantly the total rest-mass of the torus. At the end of the simulation it is conserved up to about 1%.

Tori are stable irrespective of the angular momentum distribution.

Montero, Font & Shibata (2010)

Dynamical instabilities (CACTUS/WHISKY/CARPET)

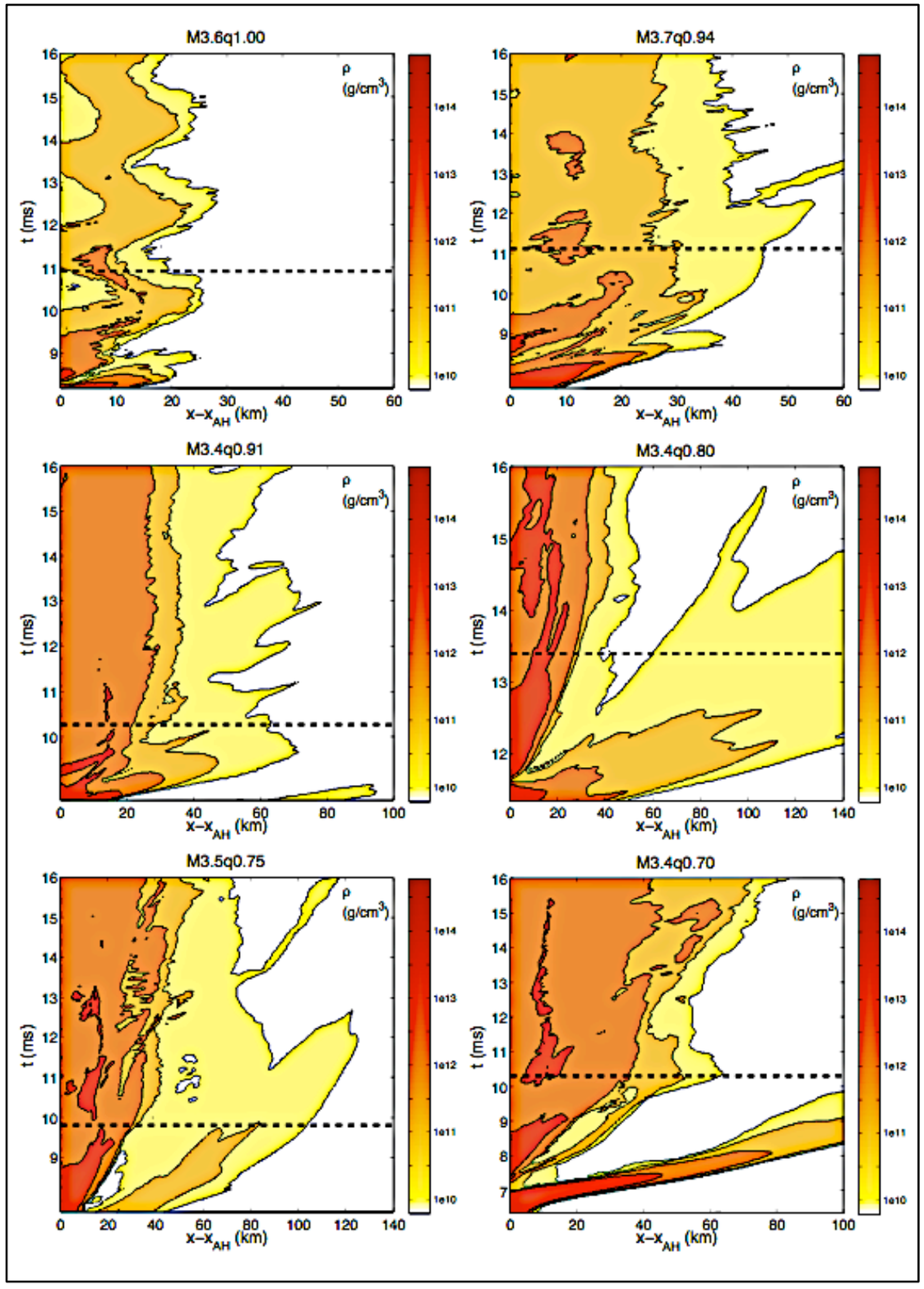

Rezzolla et al (2010)

Evolution of the rest-mass density along the positive x-axis in a frame comoving with the BH. Color-coded rest-mass density embedded in a **spacetime diagram.**

Rezolla et al (2010): All BH+torus systems formed self-consistently as the result of NS/NS mergers do not show signs of any dynamical instability, at least on the short dynamical timescales investigated.

Agreement with Montero et al (2010) even though these models are 3D and not restricted to axisymmetry.

However, on longer timescales m=1 instability may set in.

Angular velocity profiles of tori from BNS mergers

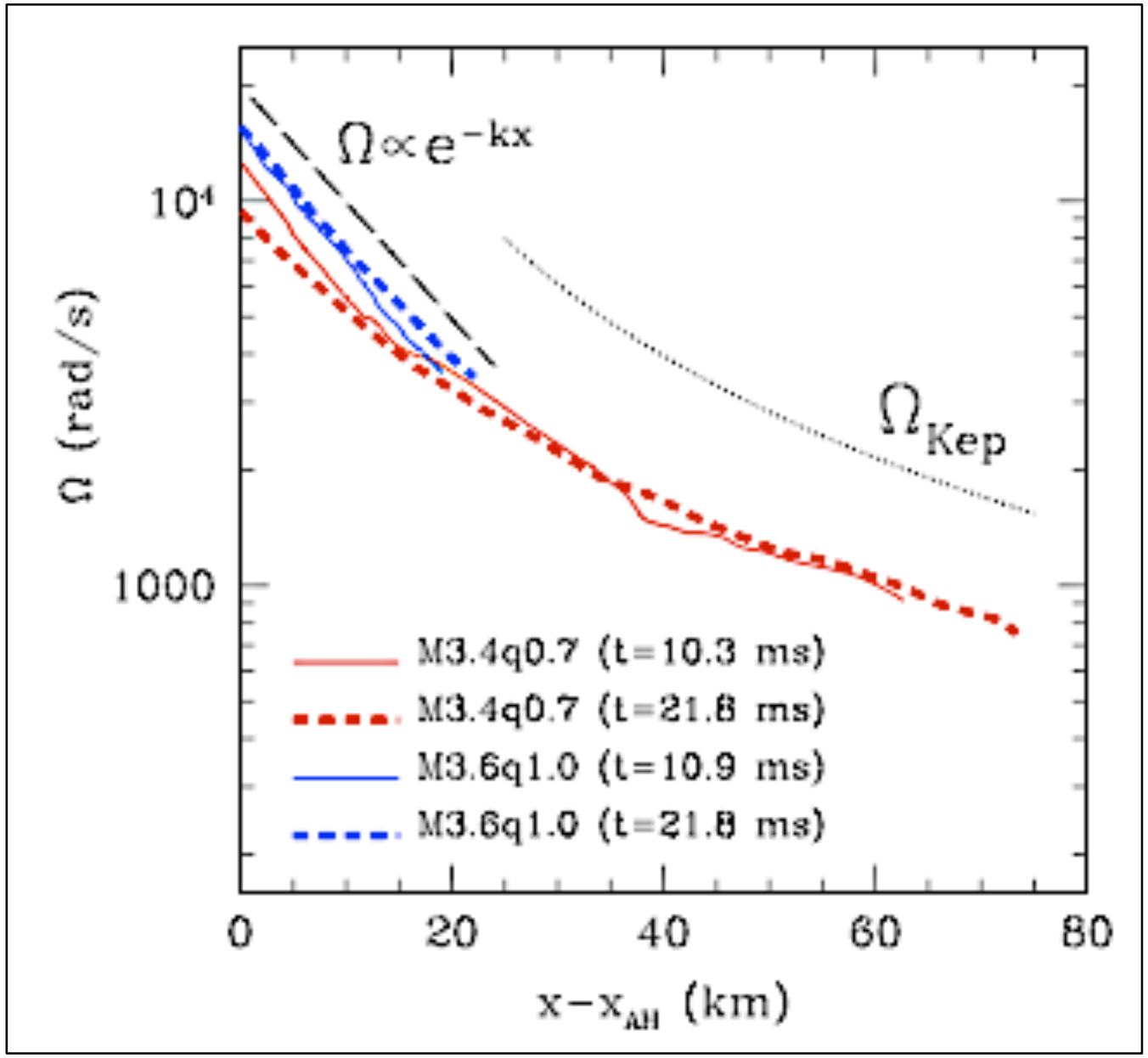

Rezzolla et al (2010)

Equal-mass binary has an exponentially decaying profile.

Unequal-mass binary reaches a **Keplerian** profile, $x^{-3/2}$. This explains the scaling of the specific angular momentum as $x^{1/2}$ and provides **firm evidence that the tori produced in this case will be dynamically stable.**

Gravitational wave emission: waveforms

Inspiral phase characterized by **harmonic oscillations** at roughly twice the orbital frequency. Increase both in amplitude and frequency.

Post-merger waveform is basically the one corresponding to the **collapse of the HMNS to a BH.**

QNM **ringdown signal** starts increasingly early for binaries with smaller mass ratios. Its signature in the waveform **less evident** due to copius mass accretion.

Besides the different amplitude evolution, the mass asymmetry also results into a **different phase evolution** which may provide information on the EOS.

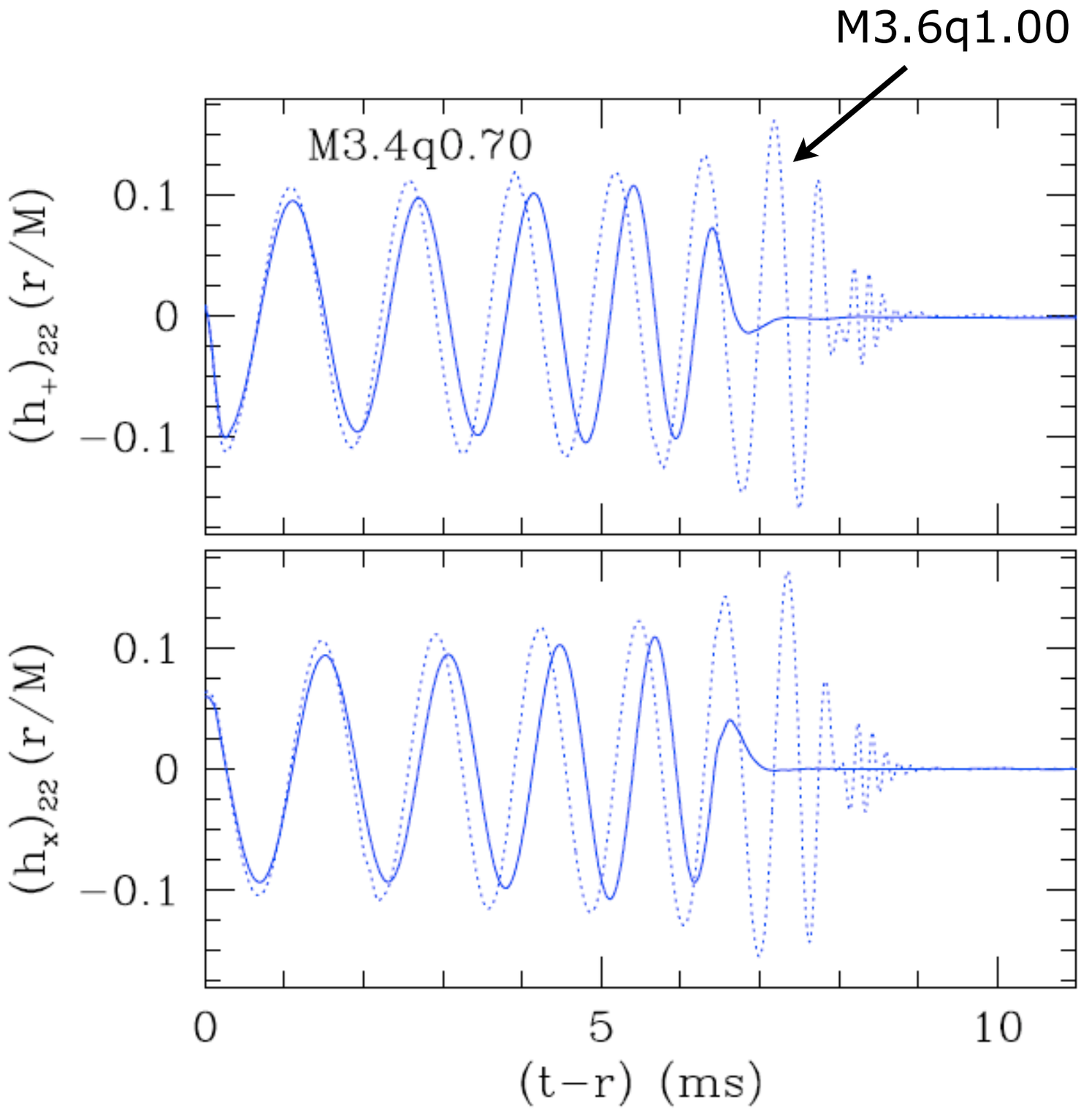

Gravitational wave emission: PSD

Power spectral densities of h+ for all models when placed @ 100Mpc.

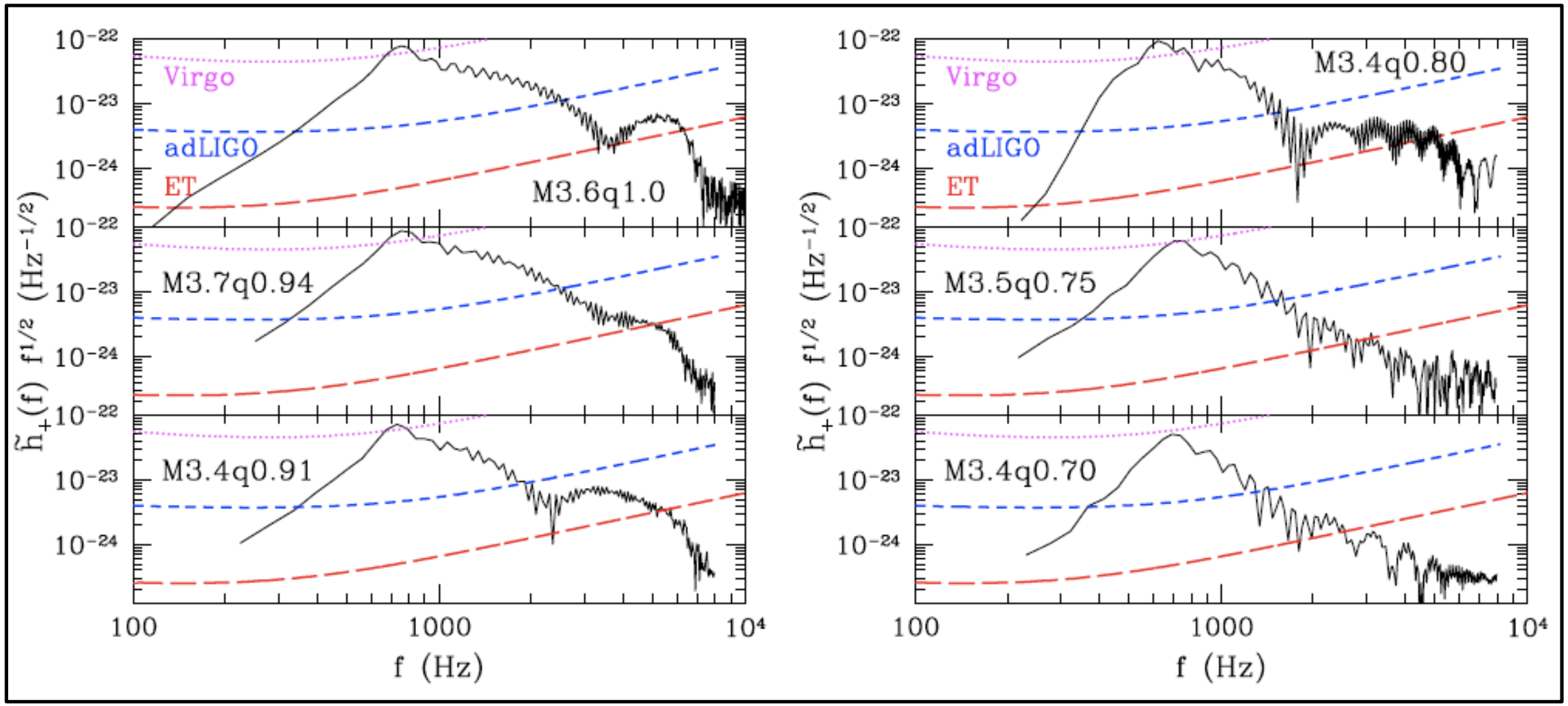

Noise curves of Virgo (magenta), advanced LIGO (blue), and Einstein Telescope (ET) (red).

Amplitude depends on the mass ratio: maximal for the high-q binaries and above the noise curve for Virgo in these cases.

New-generation detectors such as advanced LIGO will be able to reveal the inspiral signal in the frequency interval ~ 0.3 – 2.0 kHz, while essentially all of the late-inspiral and merger signal would be measured by ET.

Papaloizou-Pringle instability in tori

Using perturbation theory, **Papaloizou and Pringle (1984)** established that tori with constant specific angular momentum are unstable to non-axisymmetric global modes.

Global unstable modes have a co-rotation radius within the torus, located in a narrow region where waves cannot propagate. This region separates inner and outer regions where wave propagation is possible. Waves can tunnel through the corotation zone and interact with waves in the other region. Transmitted modes amplified only if there is a feedback mechanism, in the form of a reflecting boundary at the inner and/or outer edge of the torus.

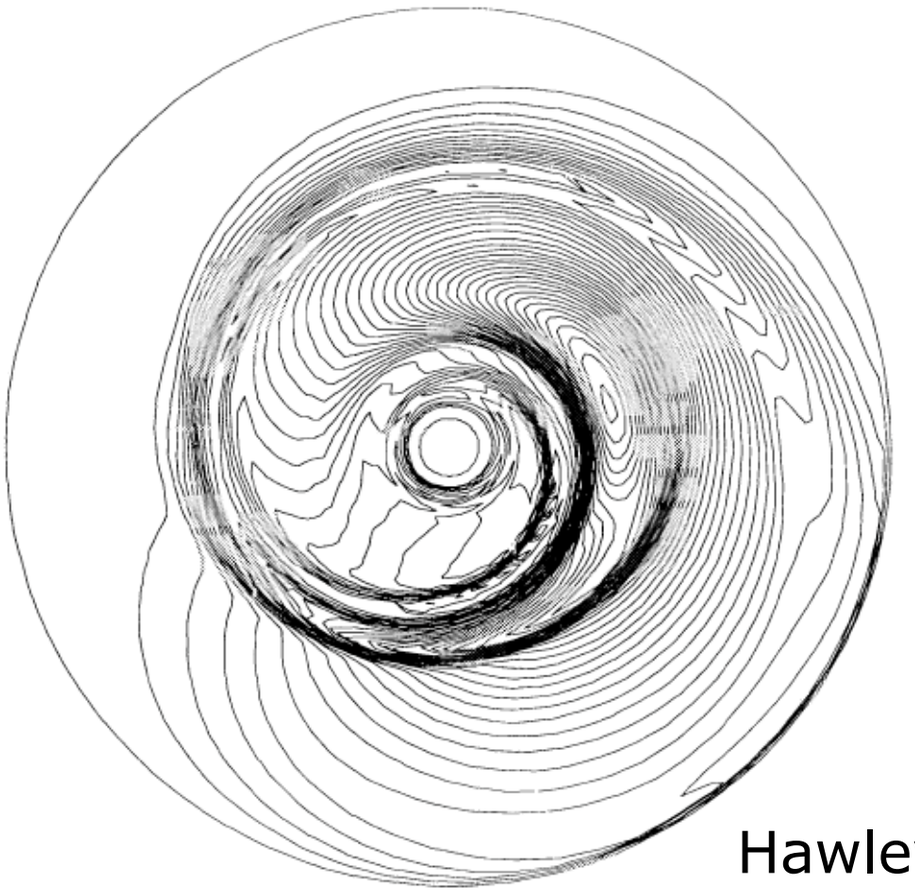

Hawley (1991)

Manifestation of the PPI: counter-rotating epicyclic vortices, or **"planets"**, with m planets emerging from the growth of a mode of order m.

Early non-linear work by Hawley, Blaes, et al. Fixed metric computations.

Recent numerical relativity work by Korobkin et al (2010): only l-constant models & short evolution times.

PPI models: initial data

Both, constant and non-constant angular momentum tori.

Model	j profile	$M_{\rm tor}/M_{\rm BH}$	$r_{\rm in}/M_{\rm BH}$	$r_{\rm c}/M_{\rm BH}$	$r_{\rm out}/M_{\rm BH}$	$t_{\rm orb}/M_{\rm BH}$	$t_{\rm sim}/t_{\rm orb}$	$\mathrm{Im}(\omega_1)/\Omega_{\rm c}$	δ_1
C2	constant (3.91)	0.20	3.2	8.15	20.0	177.2	≈ 26	0.236	≈ 0.1
C1	constant (3.83)	0.10	3.3	8.02	19.8	172.6	≈ 34	0.142	≈ 0.1
C06	constant (3.80)	0.06	3.6	8.01	19.8	171.6	≈ 40	0.089	≈ 0.1
NC2	$j \propto r^{0.29}$ (3.56)	0.20	5.0	11.3	20.0	269.6	≈ 16	0.149	≈ 0.1
NC1	$j \propto r^{0.26}$ (3.53)	0.10	4.8	10.9	19.8	257.9	≈ 36	0.056	≈ 0.25
NC06	$j \propto r^{0.29}$ (3.62)	0.06	5.0	11.7	20.0	284.0	≈ 34	—	—

growth rate ↑

Fourier amplitude @ saturation

Initial data built following the approach by Shibata (2006) and evolved using the fixed mesh refinement numerical relativity code **SACRA** (Yamamoto, Shibata & Taniguchi 2008)

Computers: XT4 @ CfCA NAOJ & NEC-SX8 @ YITP.

Animation model NC1: x-y plane

Development of the m=1 PPI.

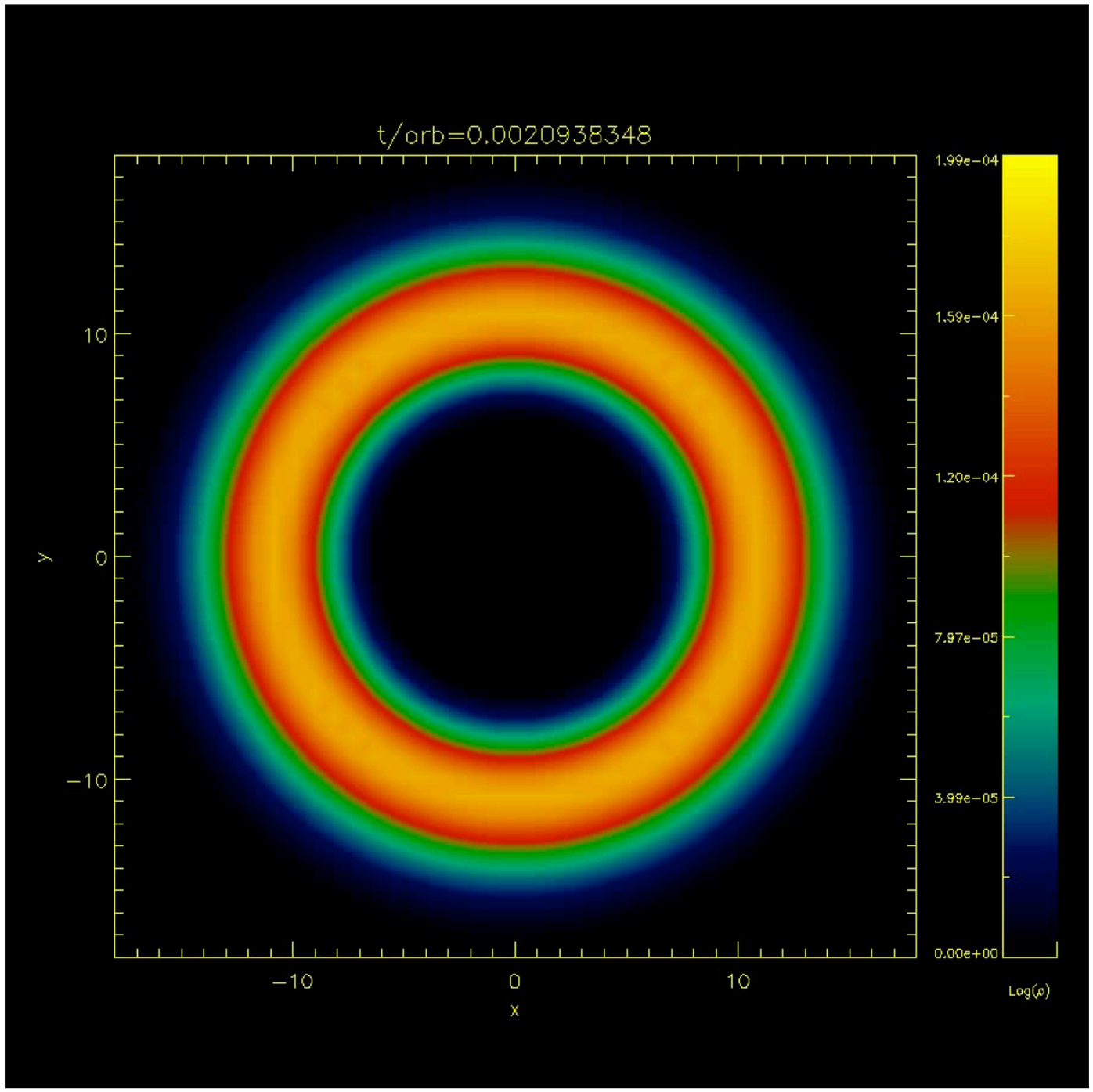

Kiuchi et al (2011)

m=1 mode grows for all j profiles

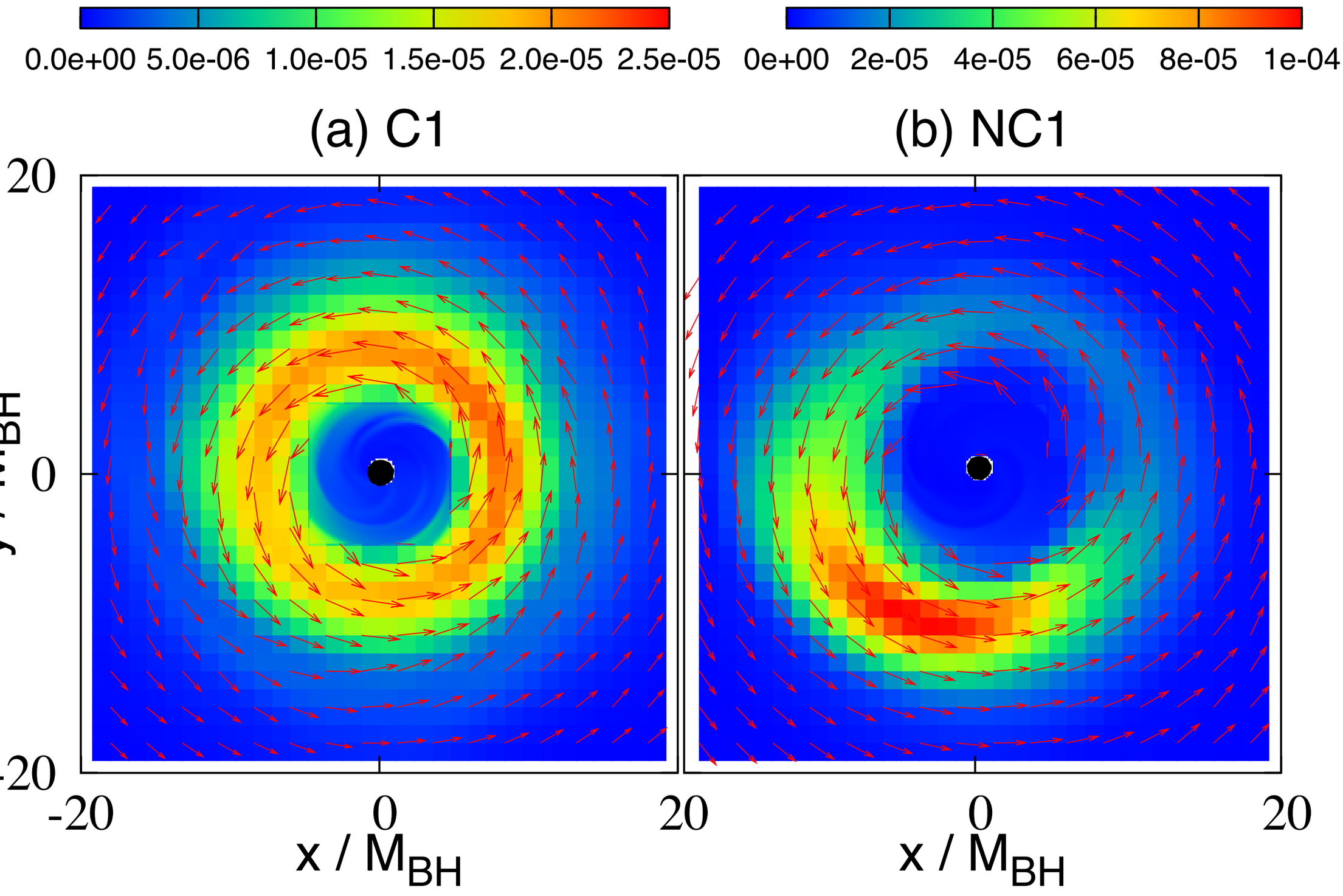

Evolution of mass-flux

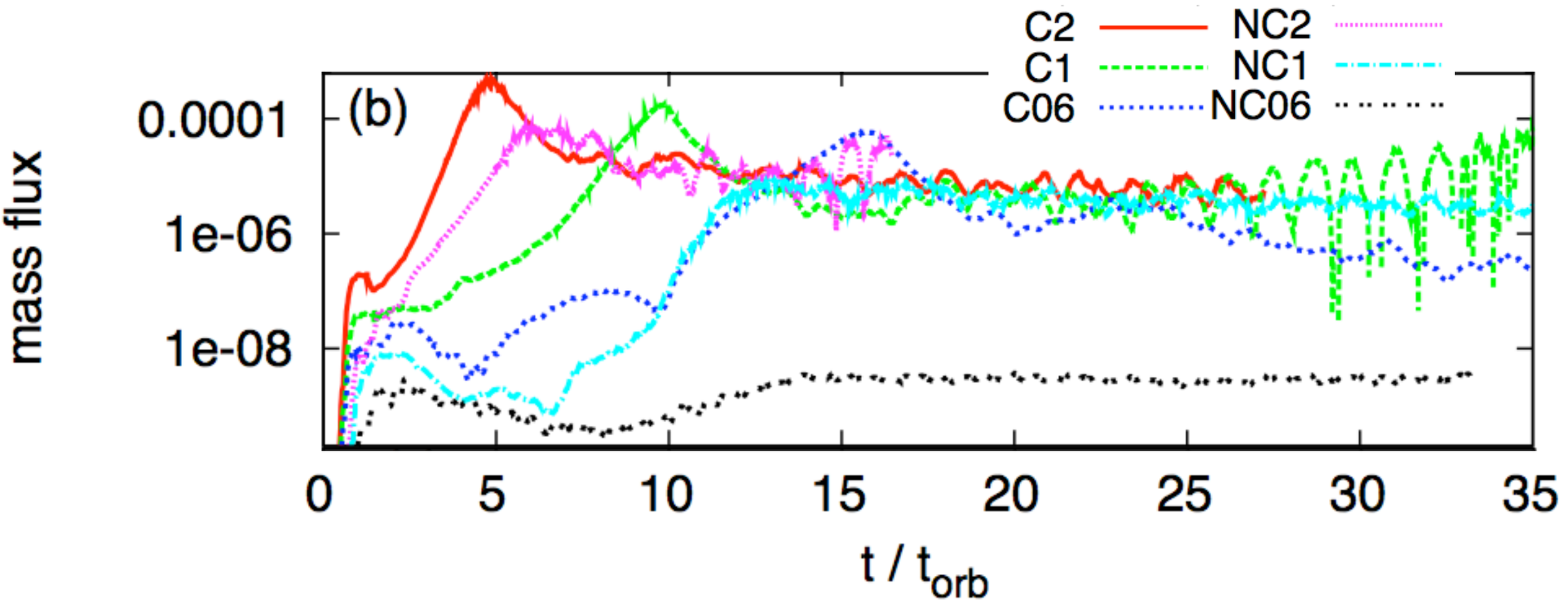

Mass flux increases exponentially with the PPI growth.

NC models show smaller mass flux at mode saturation than C models (dependence of accretion history on the j-profile).

More massive tori and/or constant j-profile favor PPI with respect to less massive tori and/or non-const j-profile (NC06 is PP-stable).

Evolution of (m=1-3) Fourier mode-amplitude

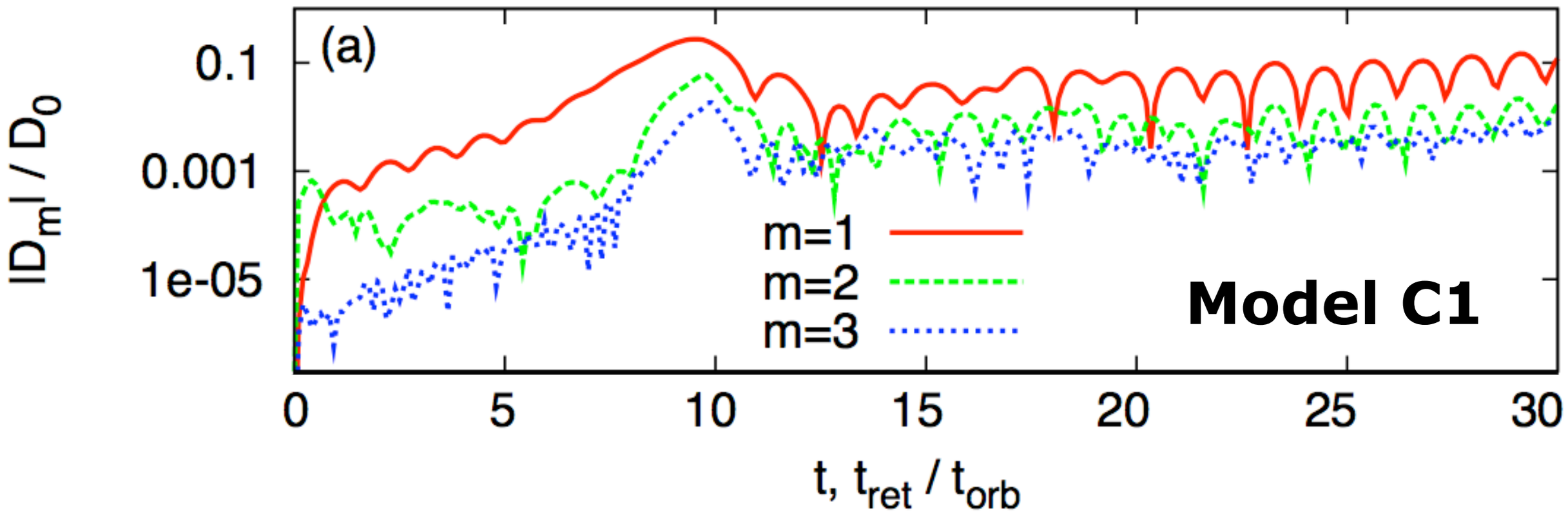

Evolution of the Fourier modes for the density perturbation of model C1.

$$D_m = \int \rho \, e^{im\varphi} \, d^3x$$

The m=1 mode is the fastest growing mode.

PPI growth rate (fit to the numerical data): $\mathrm{Im}(\omega_1)/\Omega_c = 0.236$

For all models growth rate range spans 5-25% of the angular velocity.

Massive and/or j-const models show larger growth rates (agreement with Korobkin et al (2011).

Gravitational waveform

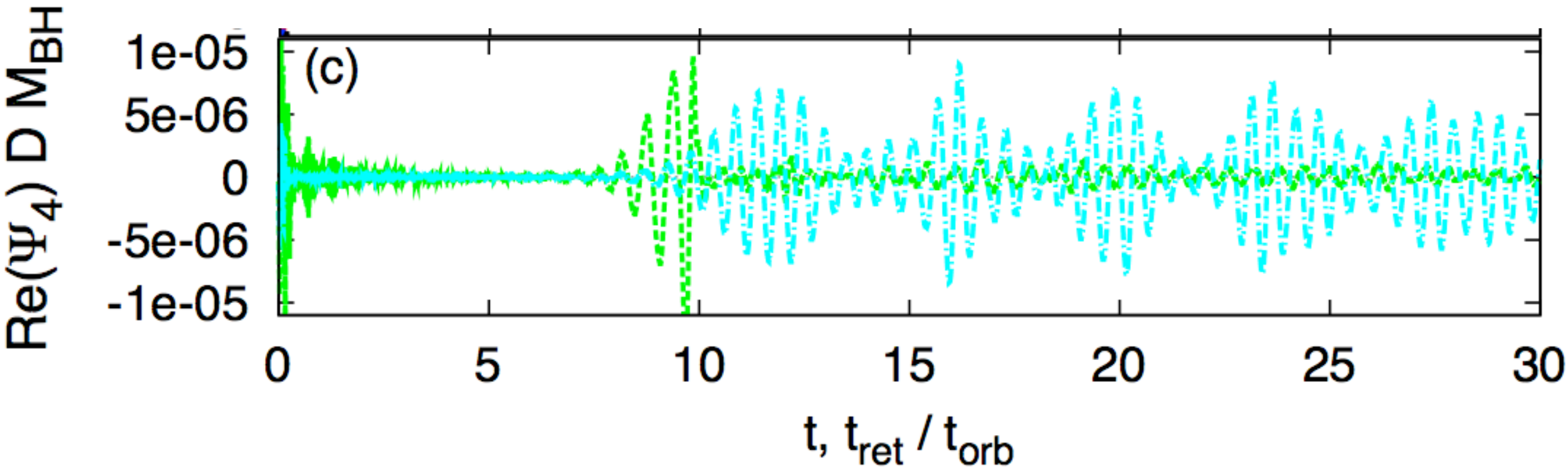

Outgoing component of the complex Weyl scalar for models **C1 (green)** and **NC1 (blue).**

Irrespective of mass ratio and rotation-law, the PPI saturates after about 10 orbital periods. Burst in GWs emitted by the PPI nonlinear growth and saturation. **After saturation, m=1 structure survives for many rotation periods and tori become good GW emitters.**

Modulation in the GW signal found for non-const j models: variability in the maximum rest-mass density and associated ***p*-mode excitation in the torus.**

Gravitational wave spectra

$M_{\rm BH} = 10^6 M_\odot,\ D = 10\,{\rm Gpc}$ $M_{\rm BH} = 10 M_\odot,\ D = 100\,{\rm Mpc}$

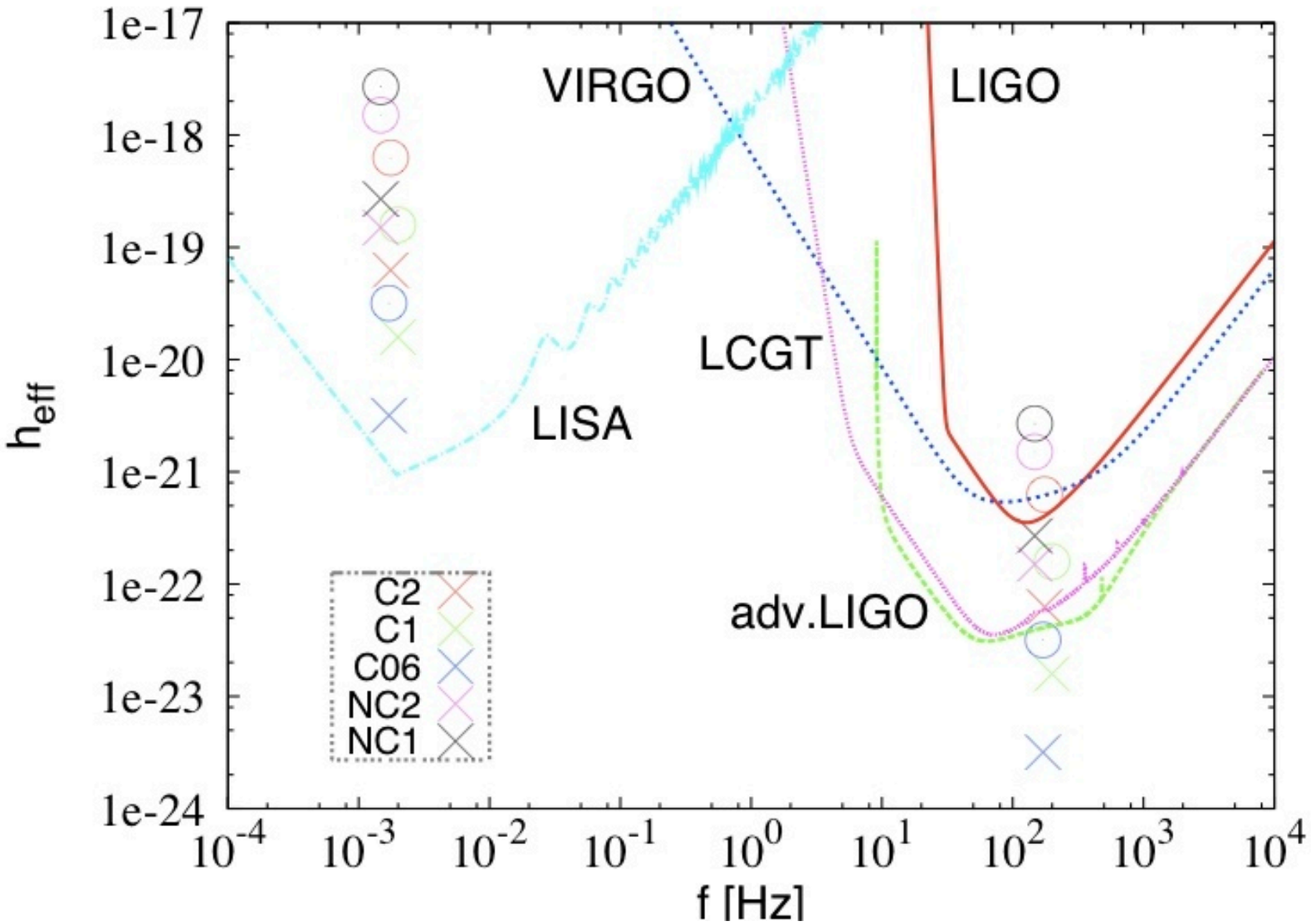

Numerical results can be rescaled for arbitrary BH mass.

X: peak amplitudes (simulations)
O: hypothetical amplitudes from accretion timescales

$t_{\rm acc} \sim 1 - 8 \times 10^4\, M_{\rm BH}$

The amplitude of the enhanced peaks could be larger than the noise level of the advanced ground-based detectors.

GWs from the SMBH scenario particularly well suited for LISA.

Summary

Numerical relativity simulations of BNS and black hole - torus systems have been presented. Focus of attention on the **gravitational waves from the merger** and on the **long-term evolution of the torus.**

Gravitational waveforms from BNS mergers show strong dependence on total mass and EOS.

Unequal mass BNS mergers lead to massive tori with masses as large as $0.1M_{tot}$.

When analyzing the evolution of the angular-momentum distribution in the tori, we find no evidence for the onset of the runaway instability. However, on longer time scales non-axisymmetric (Papaloizou-Pringle) instabilities set in, the **m=1 mode being the fastest growing mode.**

m=1 structure (planet) survives with significant amplitude well beyond the PPI nonlinear growth and saturation. **This leads to the emission of quasi-periodic gravitational waves of large amplitude.**

Advanced detectors may reveal such gravitational wave source. For stellar-mass BHs our results suggest that the so-called collapsar hypothesis of GRBs may be verified via observation of gravitational waves.